Dalton Transactions

Accepted Manuscript

This article can be cited before page numbers have been issued, to do this please use: S. Bhakat, P. Adão, S. Majumder, S. P. Dash, S. Roy, M. L. Kuznetsov, J. Costa Pessoa, C. S. B. Gomes, M. R. Hardikar, E. R.T Tiekink and R. Dinda, *Dalton Trans.*, 2018, DOI: 10.1039/C8DT01668B.

ROYAL SOCIETY OF CHEMISTRY

rsc.li/dalton

View Article Online
DOI: 10.1039/C8DT01668B

Synthesis, structure, solution behavior, reactivity and biological evaluation of oxidovanadium(IV/V) thiosemicarbazone complexes.

Saswati,[a] Pedro Adão,[b] Sudarshana Majumder,[a,c] Subhashree P. Dash,[a,d] Satabdi Roy,[a,e] Maxim L. Kuznetsov,[b] João Costa Pessoa,[b,*] Clara S. B. Gomes,[b] Manasi R. Hardikar,[f] Edward R. T. Tiekink[g] and Rupam Dinda*[a]

[a]*Department of Chemistry, National Institute of Technology, Rourkela 769008, Odisha, India*

[b]Centro de Química Estrutural, Instituto Superior Técnico, Universidade de Lisboa, Av. Rovisco Pais, 1049-001 Lisboa, Portugal

[c]*Darmstadt University of Technology, Clemens-Schöpf Institute of Organic Chemistry and Biochemistry, Alarich-Weiss Str. 4, 64287 Darmstadt, Germany.*

[d]*Department of Basic Sciences, Parala Maharaja Engineering College, Sitalapalli, Brahmapur, Odisha 761003, India*

[e]*Department of Chemistry, Indian Institute of Technology, Kanpur 208016, Uttar Pradesh, India.*

[f]*Biometry and Nutrition Group, Agharkar Research Institute, G.G. Agrakar Road, Pune 411004*

[g]*Research Centre for Crystalline Materials, School of Science and Technology, Sunway University, Bandar Sunway, Selangor Darul Ehsan 47500, Malaysia*

Abstract

The synthesis and characterization of an oxidovanadium(IV) [$V^{IV}O$(L)(acac)] (**1**) and of two dioxidovanadium(V) [$V^{V}O_2$(L´)] (**2**) and [$V^{V}O_2$(L)] (**2a**) complexes of the Schiff base formed from the reaction of 4-(*p*-fluorophenyl) thiosemicarbazone with pyridine-2-aldehyde (HL) is described. The oxidovanadium(IV) species [$V^{IV}O$(L)(acac)] (**1**) was synthesized by the reaction of $V^{IV}O(acac)_2$ with the thiosemicarbazone HL in refluxing ethanol. The recrystallization of [$V^{IV}O$(L)(acac)] (**1**) in DMF, CH_3CN or EtOH gave the same product *i.e.* the dioxidovanadium(V) complex [$V^{V}O_2$(L)] (**2a**); however, upon recrystallization of **1** in DMSO a distinct compound [$V^{V}O_2$(L')] (**2**) was formed, wherein the original ligand L^- is transformed to a rearranged one, L'^-. In the presence of DMSO the ligand in complex **1** is found to undergo methylation at the carbon centre attached to imine nitrogen (aldimine) and transformed to the corresponding $V^{V}O_2$- species through *in situ* reaction. The synthesized HL and the metal

View Article Online
DOI: 10.1039/C8DT01668B

complexes were characterized by elemental analysis, IR, UV–Vis, NMR and EPR spectroscopy. The molecular structure of $[V^{V}O_2(L')]$ (**2**) was determined by single crystal X–ray crystallography. The methylation of various other ligands and complexes prepared from different vanadium precursors under similar reaction conditions was also attempted and it was confirmed that the imine methylation observed is both ligand and metal precursor specific. Complexes **1** and **2** show *in vitro* insulin-like activity against insulin responsive L6 myoblast cells, higher than $V^{IV}O(acac)_2$, with complex **1** being more potent. In addition, the *in vitro* cytotoxicity studies of HL, and of complexes **1** and **2** against the MCF–7 and Vero cell lines were also done. The ligand is not cytotoxic and complex **2** is significantly more cytotoxic than **1**. DAPI staining experiments indicate that increase in time of incubation as well as increase of concentration of the complexes lead to increase in cell death.

Introduction

Reports of dimethylsulfoxide (DMSO) acting as a methylating agent in aromatic hydrocarbons[1a] and in N-methylation of amines[1b,c] have attracted significant attention, but DMSO is a comparatively stable molecule and has very few applications as reactant in organic reactions.[1d] The methylation of the C5 carbon of deoxycytosine nucleotide was reported to be brought about by DMSO in the presence of Fenton's reagent, where a methyl radical generated from DMSO is responsible for the methylation.[1e] Another example is the methylation of aromatic hydrocarbons by DMSO reported to take place via the methylsulfinyl carbanion generated from DMSO. [1a] DMSO was also reported to be a methylating agent for amines under catalyst free conditions.[1b]

The coordination chemistry of vanadium has attracted increasing interest, due to its biological properties, [2–9] and for the use of oxidovanadium complexes in oxidation and oxo transfer reactions catalysis,[10-16] and potential medicinal applications.[17-21] Vanadium is one of the trace bio-elements existing in the human body whose complexes have been found to show antibacterial, antitumor, insulin-enhancing and anti-parasitic effects. [17,19–21a,22-25,26] Vanadium complexes could also suppress the growth and spread of existing tumours by inhibiting tumour

View Article Online
DOI: 10.1039/C8DT01668B

cell proliferation, inducing apoptosis and limiting the invasion and metastatic potential of neoplastic cells. [19,20,25,27–28] Inorganic $V^{IV}O$- and $V^{V}O_2$-compounds, as well as some vanadium(IV)/(V) compounds, are insulin-enhancing agents [17,19,29-33] and the discovery of the *in vivo* insulin mimesis per os of oxidovanadates(V),[34] of the oxidovanadium(IV)- ($V^{IV}O$-) precursor, $V^{IV}OSO_4$,[35] and of the more potent bis(maltolato)-oxidovanadium(IV) (BMOV) [30,32,36,37] encouraged exploration of vanadium complexes for the treatment of type II diabetes, as well as many attempts to understand the mechanisms of action. [30,32,37-41] Thus, several different approaches have been used to develop orally active vanadium containing insulin enhancing agents.[32,33,41,42,43]

Thiosemicarbazones are an important class of compounds that have considerable pharmacological interest due to their antibacterial, anti-viral, anti-malarial, anti-leprotic, anti-tumor and anti-cancer activities.[44–47] Metal complexes of thiosemicarbazone ligands have shown variable bonding properties and structural diversity, along with promising biological applications and ion sensing abilities.[48–59]

Keeping these factors in mind and in applying our expertise in oxidovanadium chemistry, [60] herein we report the formation of an oxidovanadium(IV) complex $[V^{IV}O(L)(acac)]$ (**1**) ($acac^-$ = acetylacetonato) derived from the Schiff base formed by the condensation of 4-(*p*-fluorophenyl)thiosemicarbazone with pyridine-2-aldehyde (HL), which gradually oxidizes to the dioxidovanadium(V) complex $[V^{V}O_2(L')]$ (**2**) upon standing in DMSO solution, with an unprecedented methylation of the aldimine carbon in the ligand backbone (Scheme 1). No such methylation occurs upon recrystallization of **1** in other solvents such as DMF, CH_3CN, EtOH, where $[V^{IV}O(L)(acac)]$ (**1**) undergoes oxidation to $[V^{V}O_2(L)]$ (**2a**), with no modification in the ligand.

The synthesized ligand and the metal complexes were characterized by elemental analysis, IR, UV–Vis, NMR and EPR spectroscopy. The molecular structure of $[V^{V}O_2(L')]$ (**2**) was also determined by single crystal X–ray diffraction crystallography (XRD). The outline of the process of formation of the methylated oxidovanadium(V) complex **2** is tentatively explained and further supported by DFT calculations. In addition, from the comparative study of various other ligands and complexes prepared from different vanadium precursors in similar reaction conditions, it was fortified that the imine methylation observed is both ligand and metal precursor specific for this system.

Complexes **1** and **2** were assayed for their *in vitro* insulin-like activity against insulin responsive L6 myoblast cells. Results indicate both complex **1** and **2** to exhibit considerable insulin-like activity, higher than $V^{IV}O(acac)_2$, with **1**

View Article Online
DOI: 10.1039/C8DT01668B

being more potent than **2**. In addition, the *in vitro* toxicity studies of **1** and **2** against MCF–7 (breast cancer cells) and Vero cells (noncancerous mammalian cells) were also assayed and complex **1** was found to have higher cytotoxicity towards both cell lines. Results of DAPI staining experiments carried out indicated that increase in time of incubation and/or increase of concentration of complexes **1** and **2** lead to increase in cell death.

Experimental Section

Materials and methods

$[V^{IV}O(acac)_2]$, where $acac^-$ is acetylacetonate, was prepared as described in the literature.[61] Reagent grade solvents were dried and distilled prior to use. All other chemicals were of reagent grade, available commercially and used as received. HPLC grade DMSO and CH_3CN were used for spectroscopic and electrochemical studies, and ethanol or methanol were used for synthesis of ligands and metal complexes. Commercially available TEAP (tetraethylammonium perchlorate) was properly dried and used as a supporting electrolyte for recording cyclic voltammograms of the complexes. Elemental analyses were made on a Vario ELcube CHNS Elemental analyzer. IR spectra were recorded on a Perkin-Elmer Spectrum RXI spectrometer. ^1H and ^{13}C NMR spectra were recorded with a Bruker Ultrashield 400 MHz spectrometer using $SiMe_4$ as an internal standard and ^{51}V NMR spectra were obtained on a Bruker Avance III 400 MHz spectrometer and chemical shift ^{51}V values (δ_V) were referenced relative to neat V^VOCl_3 as external standard. Electronic spectra were recorded on a Lamda 25, Perkin Elmer spectrophotometer. Electrochemical data were collected using PAR Versastat-II instrument driven by E-chem software (PAR) at 298 K in a dry nitrogen atmosphere. Cyclic voltammetry experiments were carried out with Pt working and auxiliary electrodes and Ag/AgCl as reference electrode. EPR spectra were recorded with a Bruker EMX X-band spectrometer either at 77 K or at room temperature. X-band EPR measurements were carried out on a JEOL JES-FA 200 and Bruker EMX EPR Spectrometer. The mass spectrometer used is an ion trap equipped with an ESI ion source (Thermo Scientific). The mass spectrometer was operated in the ESI positive and negative ion modes, with the following optimized parameters: ion spray voltage, + 4/ -5.3 kV; capillary voltage, 5/-20 V; tube lens offset, 63/-124; sheath gas (N2), 20 arbitrary units; capillary temperature 275 ºC. The spectra, typically correspond to the average of 20-30 scans, and were normally recorded in the range 100-2000 Da. MCF–7 cells (a human breast adenocarcinoma cell line) and Vero cells (noncancerous mammalian cells, to check the effect of the complexes on the noncancerous cells) were obtained from the National Centre of Cell Science (NCCS), Pune, India and were maintained in minimal essential medium supplemented with 10% fetal bovine serum (FBS), penicillin-streptomycin solution and incubated at 37°C in 5% CO_2 and 95% humidified incubator.

Synthesis of ligand (HL)

View Article Online
DOI: 10.1039/C8DT01668B

The thiosemicabazide was prepared from distilled *p*-fluoroaniline by a method reported earlier.[62] The Schiff base ligand, 4-(*p*-fluorophenyl) thiosemicarbazone of pyridine-2-aldehyde, was prepared in 80–90% yield by stirring an equimolar ratio of the thiosemicabazide with pyridine-2-aldehyde in methanol medium by standard procedures.[63] The resulting compound was filtered, washed thoroughly with methanol and dried over fused $CaCl_2$.

HL: Yield: 85%. Anal. calc. for $C_{13}H_{11}N_4SF$: C, 56.92; H, 4.04; N, 20.42. Found: C, 56.95; H, 4.00; N, 20.41. Main IR peaks (KBr, cm^{-1}, atom numbering is depicted in Scheme 1): ν(N(1)–H), 3311 s; ν(N(2)–H), 2967 s; *ν*(C(8)–H), 2825 m; ν(C=C), 1638 s; ν(C(7)–S(1)), 836 s. ^{1}H NMR (DMSO–d_6, 400 MHz, ppm): δ_H: 12.08 (s, 1H, N(1)H), 10.29 (s, 1H, N(2)H), 8.59 (s, 1H, C(8)H), 8.58–7.20 (m, 8H, C_6H_4). ^{13}C NMR (DMSO-d_6, 100 MHz, ppm): δ_c: 177.25, 161.46, 159.05, 153.58, 149.82, 143.62, 136.98, 135.77, 128.86, 128.77, 124.76, 121.12, 115.37.

Synthesis of [$V^{IV}O$(L)(acac)] (1)

To a solution of HL (0.274 g, 0.100 mmol) in hot ethanol, $V^{IV}O(acac)_2$ (0.265 g, 1.0 mmol) was added. The mixture was refluxed for 2 h, yielding a dark green color crystalline precipitate of [$V^{IV}O$(L)(acac)] (**1**): Yield: 75%. Anal. calc. for $C_{18}H_{17}FN_4VO_3S$: C, 49.21; H, 3.90; N, 12.75. Found: C, 49.24; H, 3.87; N, 12.73. Main solid state IR peaks (KBr, cm^{-1}): ν(N(1)–H), 3317 s; ν(C=C), 1602 s; ν(V=O), 949 s; ν(C(7)–S(1)), 762 s. Spin Hamiltonian parameters determined from EPR spectra at 77 K: $g_{x,y}$ =1.978, g_z=1.952, $|A_{x,y}|$ = 51.9×10^{-4} cm^{-1}, $|A_z|$ = 153.2×10^{-4} cm^{-1}, if the spectrum is simulated as having tetragonal symmetry. Assuming the x and y axis are not equivalent: $g_{x,y}$ =1.977 , $g_{x,y}$ =1.981, g_z=1.95, $|A_{x,y}|$ =51.1 ×10^{-4} cm^{-1}, $|A_{x,y}|$ = 52.6×10^{-4} cm^{-1}, $|A_z|$ = 152.9×10^{-4} cm^{-1}.

Synthesis of [$V^{V}O_2$(L´)] (2)

The dark green crystalline [$V^{IV}O$(L)(acac)] (**1**) was dissolved in DMSO at 60^{o}C (ca. 25 mM) and allowed to evaporate at room temperature (ca. 22 – 27 ^{o}C) for recrystallization. Reddish brown crystals were obtained from DMSO after 15 days.

[$V^{V}O_2$(L´)] (2): Yield: 65%. Anal. calc. for $C_{14}H_{12}FN_4VO_2S$: C, 45.41; H, 3.27; N, 15.13. Found: C, 45.43; H, 3.25; N, 15.16. Main IR peaks (KBr, cm^{-1}): ν(N(1)–H), 3268 s; ν(C=C), 1604 s; ν(V=O), 937, 925 s; ν(C(7)–S(1)), 765 s. ^{1}H NMR (DMSO–d_6, 400 MHz, ppm): δ_H: 10.20 (s, 1H, N(1)H), 8.72–7.18 (m, 8H, C_6H_4), 2.66 (s, 3H, C(8)H_3). ^{13}C NMR (DMSO-d_6, 100 MHz, ppm): δ_c: 154.34, 153.80, 143.72, 141.34, 137.23, 130.68, 129.12, 126.94, 125.35, 122.48, 122.40, 115.88, 115.65, 67.87. ^{51}V NMR (DMSO–d_6, ppm) δ_v: -434, -577.

Synthesis of [$V^{V}O_2$(L)] (2a)

View Article Online
DOI: 10.1039/C8DT01668B

The dark green crystalline residue of [$V^{IV}O$(L)(acac)] (**1**) was dissolved in EtOH (ca. 25 mM) for recrystallization and allowed to evaporate at room temperature (ca. 22 – 27 ^{o}C). A yellow residue of the complex was obtained after few days. Similar results were obtained when recrystallization of **1** was done in CH_3CN and DMF.

[$V^{V}O_2$(L)] (2a): Yield: 70%. Anal. calc. for $C_{13}H_{10}FN_4VO_2S$: C, 43.83; H, 2.83; N, 15.73. Found: C, 43.80; H, 2.85; N, 15.76. Main IR peaks (KBr, cm^{-1}): ν(N(1)–H), 3256 s; *ν*(C(8)–H), 2834 m; ν(C=C), 1589 s; ν(V=O), 934, 922 s; ν(C(7)–S(1)), 775 s. ^{1}H NMR (DMSO–d_6, 400 MHz, ppm): δ_H 10.29 (s, 1H, N(1)H), 8.79 (s, 1H, C(8)H), 8.78–7.16 (m, 8H, C_6H_4). ^{13}C NMR (DMSO-d_6, 100 MHz, ppm): δ_c 166.16, 160.28, 159.10, 156.73, 150.24, 149.31, 138.11, 137.27, 125.45, 119.96, 119.88, 116.29, 116.06. ^{51}V NMR (DMSO–d_6, ppm) δ_v: -434.

[N-(4-fluorophenyl)-5-(pyridin-2-yl)-1,3,4-thiadiazol-2-amine] (3)

The compound [$V^{V}O_2$(L)] **(2a)** was dissolved in DMSO (ca. 25 mM) and the solution kept at 60 ^{o}C. There was no change in colour but there was a significant alteration to the ^{1}H NMR spectrum after 5 days under these conditions (Figs. 10 and S15). After cooling the reaction mixture and letting it stand at room temperature, a crystalline material slowly formed after approximately a week. The obtained crystalline product corresponds to a cyclized and oxidized compound **3** (Fig. S1), which was characterized by single-crystal x-ray diffraction.

Computational Details

The full geometry optimization of the molecular structures was carried out at the DFT level of theory using B3P86 functional[64] with the help of the Gaussian-09 program package.[65] This functional was found to be sufficiently accurate for the theoretical studies of structural parameters and ^{51}V NMR chemical shifts of various V complexes.[66] No symmetry operations were applied for any of the structures calculated. The geometry optimization was carried out using a relativistic Stuttgart pseudopotential which describes 10 core electrons and the appropriate contracted basis set (8s7p6d1f)/[6s5p3d1f] for the vanadium atom[67] and the 6-31G* basis set for other atoms. The Hessian matrix was calculated analytically for the optimized structures to prove the location of correct minima (no imaginary frequencies) and to estimate the thermodynamic parameters, the latter being calculated at 25 °C.

The total energies corrected for solvent effects E_s were estimated at the single-point calculations on the basis of gas-phase geometries at the IEFPCM-B3P86/6-311+G*//gas-B3P86/6-31G* level of theory using the polarizable continuum model in the IEFPCM version[68] with DMSO as the solvent. The UAKS model was applied for the molecular cavity with dispersion,

View Article Online
DOI: 10.1039/C8DT01668B

repulsion and cavitation contributions. The entropic term in DMSO solution (S_s) was calculated according to the procedure described by Wertz[69a] and Cooper and Ziegler[69b] using eqn (1)–(4):

$$\Delta S_1 = R \ln V^s_{m,liq} / V_{m,gas} \quad (1)$$

$$\Delta S_2 = R \ln V^\circ_m / V^s_{m,liq} \quad (2)$$

$$\alpha = \frac{S^{\circ,s}_{liq} - (S^{\circ,s}_{gas} + R \ln V^s_{m,liq} / V_{m,gas})}{(S^{\circ,s}_{gas} + R \ln V^s_{m,liq} / V_{m,gas})} \quad (3)$$

$$S_s = S_g + \Delta S_{sol} = S_g + [\Delta S_1 + \alpha(S_g + \Delta S_1) + \Delta S_2] =$$

$$S_g + [(-11.60 \text{ cal/mol·K}) - 0.27(S_g - 11.60 \text{ cal/mol·K}) + 5.25 \text{ cal/mol·K}] \quad (4)$$

where S_g is the gas-phase entropy of the solute, ΔS_{sol} is the solvation entropy, $S^{\circ,s}_{liq}$, $S^{\circ,s}_{gas}$ and $V^s_{m,liq}$ are the standard entropies and molar volumes of the solvent in the liquid or gas phases (188.8 and 306.7 J/mol·K and 71.03 mL/mol, respectively, for DMSO), $V_{m,gas}$ is the molar volume of the ideal gas at 25 °C (24450 mL/mol), V°_m is the molar volume of the solution that correspond to the standard conditions (1000 mL/mol). The enthalpies and Gibbs free energies in solution (H_s and G_s, respectively) were estimated using equations 5 and 6

$$H_s = E_s(6\text{-}311+G^*) + H_g(6\text{-}31G^*) - E_g(6\text{-}311+G^*) \quad (5)$$

$$G_s = H_s - TS_s \quad (6)$$

where E_s and E_g are the total energies in solution and the gas phase and H_g is the gas-phase enthalpy calculated at the corresponding level.

Magnetic shielding was calculated for the equilibrium geometries using the GIAO method[70] at the IEFPCM-B3P86/6-311+G(2d,p)//6-31G(d) level. The ^{51}V chemical shifts were estimated relative to V^VOCl_3, calculated at the same level of theory. The ^{51}V hyperfine coupling constants were estimated at the single-point calculations using the BHandHLYP functional and 6-311G* basis set for all atoms on the basis of the equilibrium geometry obtained at the B3P86/6-31G*(V-ECP) level of theory. The anisotropic ^{51}V hyperfine coupling constants A_x, A_y, and A_z were estimated as the sum of the isotropic Fermi contact term and corresponding dipolar hyperfine interaction term.[71] It must be emphasized that for a V^{IV}-species the hyperfine coupling constant (A) values may be negative, but in the literature normally it is their absolute value that is reported. This simplification was also adopted in this work. Previously, it was found that half-and-half functionals such as BHandHLYP demonstrate better performance in the calculations of EPR parameters than many other hybrid functionals due to more accurate estimates of the Fermi contact term.[71a-b] Atomic charges were calculated using the natural bond orbital (NBO) partitioning scheme. [72]

View Article Online
DOI: 10.1039/C8DT01668B

X-ray crystallography

Intensity data for and **2** (295 K) were measured on an Agilent Technologies SuperNova Dual CCD with an Atlas detector fitted with Mo Kα radiation (λ = 0.71073 Å). Data processing and absorption corrections were accomplished with CrysAlis PRO.[73] Intensity data for **3** (293 K) were collected on a Bruker AXS-KAPPA APEX II diffractometer fitted with Mo Kα radiation (λ = 0.71073 Å). Data processing was carried out with SMART and SAINT,[74a] and the absorption correction was accomplished with SADABS.[74b] The structures were solved by direct methods with SHELXS-97 (**2**)[75a] and SIR2014 (**3**),[75b] and refinement (anisotropic displacement parameters (ADP's) with C-bound H atoms in the riding model approximation and a weighting scheme of the form $w = 1/[\sigma^2(F_o^2) + (aP)^2 + bP]$ for $P = (F_o^2 + 2F_c^2)/3$) was on F^2 by means of SHELXL-2014/7.[75c] The N-bound H atoms were refined with the distance constraint N–H = 0.88(1) Å. For **2**, disorder was evident in the fluorobenzene ring and this was modeled over two positions of equal weight; the dihedral angle between the two orientations is 4(1)°. Each benzene ring was constrained to be an ideal hexagon and, due to the near-overlap of the atoms, equivalent pairs were constrained to have identical ADP's. The data for **3** was less than optimal but, the structure determined unambiguously without any unusual features. Crystallographic data and final refinement details are given in Table 1. The molecular structure diagrams were drawn using ORTEP-3 for Windows[76a] at the 35% probability level and the remaining crystallographic figures were drawn with DIAMOND[76b] using arbitrary spheres. Data manipulation and interpretation were with WinGX[76a] and PLATON.[77]

Table 1 Crystal data and structure refinement details for **2** and **3**.

Compound	**2**	**3**
Formula	$C_{14}H_{12}FN_4O_2SV$	$C_{13}H_9FN_4S$
Formula weight	370.28	272.30
Color, habit	Yellow, prism	Orange, prism
Size mm	0.05 × 0.05 × 0.25	0.10 x 0.12 x 0.20
Crystal system	Monoclinic	Monoclinic
Space group	*C*2/*c*	$P2_1/c$
Unit cell dimensions		
a (Å)	19.600(3)	10.8207(16)
b (Å)	14.7000(8)	17.650(3)
c (Å)	14.922(2)	13.3819(19)
a (º)	90	90
β (º)	134.83(3)	99.691(5)
g (º)	90	90

View Article Online
DOI: 10.1039/C8DT01668B

Volume (Å^3)	3049.1(17)	2519.3(7)
Z/*Z*'	8/1	8/2
Calculated density (g cm^{-3})	1.613	2519.3(7)
Radiation	Mo Kα	Mo Kα
Absorption coefficient (mm^{-1})	0.812	1.436
F(000)	1504	1120
Theta range for data collection (º)	2.7 – 29.4	2.3 – 25.7
Reflections collected / unique	12030 / 3723	43705 / 4590
R_{int}	0.040	0.131
Data (*I*>2□(*I*)) / restraints/ parameters	2197 / 38 / 210	2246 / 2 / 349
Goodness-of-fit on F^2	1.01	1.03
Final *R*, *wR* indices [*I*>2σ(*I*)]	0.053, 0.121	0.110, 0.305
Final *R*, *wR* indices [all data]	0.101, 0.149	0.204, 0.385
a, *b* wght scheme	0.059, 3.139	0.156, 12.576
Residual electron density peaks (eÅ^{-3})	-0.27, 0.41	-0.47, 0.56

In vitro Glucose uptake assay on L6 myotubes.

L6 myoblast were cultured in DMEM containing 10% FBS and penicillin (100 U/mL) and streptomycin (100 µg/mL) in a humidified 5% CO_2 incubator at 37°C. To differentiate to myotubes, the myoblast cells (5x10^4) were seeded in 24 well plates in DMEM containing 2% FBS. The myoblast cells (5x10^4) were grown for 11 days in 0.4 mL of 2% FBS/DMEM to allow the formation of myotubes. The medium was changed every 2 days. On the 11th day, the cells were washed and incubated in Kreb's bicarbonate buffer (KRBB) for 2 h. Myotubes were then further cultured in KRBB containing 25 mM glucose along with 25, 50, 100 µM of vanadium compounds ([V^{IV}O(L)(acac)] (**1**), [V^{V}O$_2$(L´)] (**2**) and V^{IV}O(acac)$_2$) for 4 h. Insulin (2 µM) was taken as positive control.[78a] The residual glucose in the buffer aliquots remaining in each well after 4 h was estimated using hexokiase method by Randox autoanalyser.

Cytotoxicity studies.

The effect of complexes **1** and **2** on the MCF–7 cells (a human breast adenocarcinoma cell line) and Vero cells (noncancerous mammalian cells) was studied using the MTT (3-(4,5-dimethylthiazol-2-yl)-2,5-diphenyltetrazolium bromide) dye reduction assay, by measuring the optical density at 595 nm using a micro plate reader spectrophotometer. The cells were maintained in

View Article Online
DOI: 10.1039/C8DT01668B

minimal essential medium supplemented with 10% FBS, penicillin-streptomycin solution and incubated at 37°C in 5% CO_2 and 95% humidified incubator. After the cells being grown for 24 h to a subconfluent state (~ 60–70%), they were treated with different concentrations of [$V^{IV}O(L)(acac)$] (**1**) and [$V^{V}O_2(L')$] (**2**) (5, 50, 100, 200 μM) in culture medium. The complexes were dissolved in DMSO and working solutions were prepared by diluting the stock of 5 mM of each compound with plain DMEM. Final working concentration of DMSO in assay was less than 2%. The samples were tested in triplicates. After 24, 48 and 72 h the effect of the compound on cell viability was examined by the MTT test. Optical density was measured at 595 nm using an automatic microplate reader.

DAPI staining.

DAPI (4′,6-diamidino-2-phenylindole dihydrochloride) staining was carried out to examine the morphology of the nuclei after treatment. The cells were grown in the 96–well plates. After reaching approximately 90% confluency the cells were treated with [$V^{IV}O(L)(acac)$] (**1**) and [$V^{V}O_2(L')$] (**2**) at different concentrations (5, 50 100, 200 μM), and were incubated for 24, 48 and 72 h. Cells were observed with inverted fluorescence microscope after treatment to check for morphological changes, during cell death. Then the cells were washed twice with PBS (pH 7.4) and 3.7% of paraformaldehyde was added and incubated for 15 min. The cells were again washed twice with PBS and treated with 0.2% triton–X 100 and 2% BSA in PBS for 30 seconds. Again the cells were washed twice with PBS and DAPI was added and kept for 30 min in the dark. Finally, the cells were washed twice with PBS and imaged under fluorescence microscope (FLoiD, Life technologies).

Results and discussion

Synthesis

Scheme 1 illustrates the formation of the oxidovanadium(IV) complex, [$V^{IV}O(L)(acac)$] (**1**), and the dioxidovanadium(V) complexes [$V^{V}O_2(L')$] (**2**) and [$V^{V}O_2(L)$] (**2a**). The spectroscopic data are consistent with the proposed formulations. The purity of these compounds was confirmed by elemental analyses. All complexes were soluble in EtOH, CH_3CN, DMF and DMSO.

View Article Online
DOI: 10.1039/C8DT01668B

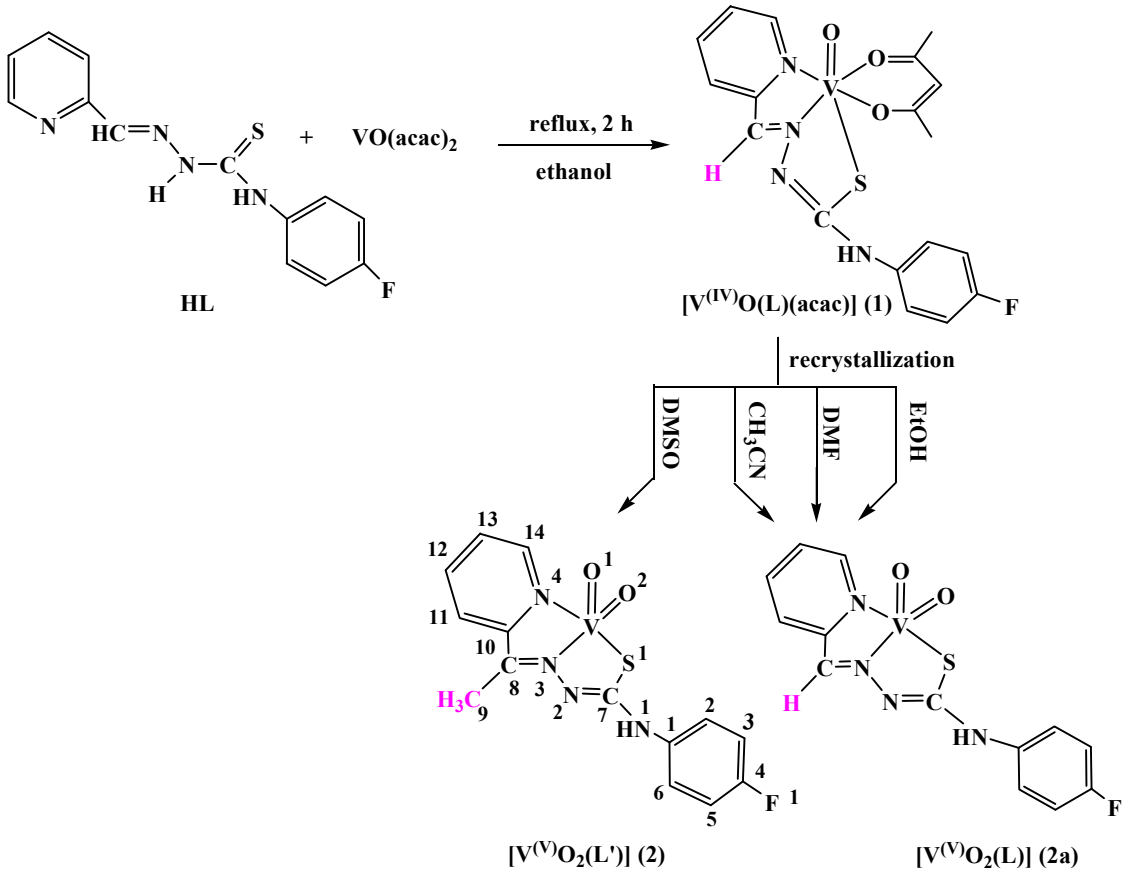

Scheme 1 Schematic representation of HL and outline of the processes to obtain $[V^{IV}O(L)(acac)]$ (**1**), $[V^{V}O_2(L')]$ (**2**) and $[V^{V}O_2(L)]$ (**2a**).

The processes take place in two steps: firstly, the formation of $[V^{IV}O(L)(acac)]$ (**1**) from the reaction of $[V^{IV}O(acac)_2]$ with HL {4-(*p*-fluorophenyl)thiosemicarbazone of pyridine-2-aldehyde}. Then, in presence of DMSO, there is aerial oxidation of $[V^{IV}O(L)(acac)]$ (**1**) to form the $V^{V}O_2$-complex $[V^{V}O_2(L')]$ (**2**), which contains a rearranged ligand L'^{-} where methylation of an aldimine carbon has taken place. However, in the presence of other solvents such as DMF, CH_3CN and EtOH no such ligand change is observed and the corresponding $V^{V}O_2$-compound $[V^{V}O_2(L)]$ (**2a**) is formed from $[V^{IV}O(L)(acac)]$ (**1**). The reaction of **2a** with

View Article Online
DOI: 10.1039/C8DT01668B

DMSO was also carried out at 60 °C; however, in that case there was no change in colour of the reaction mixture or methylation at the aldimine C atom.

Plausible pathways for the alkylation of complex 1 in the presence of DMSO

Scheme 2 depicts pathways A and B that can be proposed for the formation of the methylated product $[V^{V}O_2(L')]$ (**2**) from the $V^{IV}O$-complex $[V^{IV}O(L)(acac)]$ (**1**).

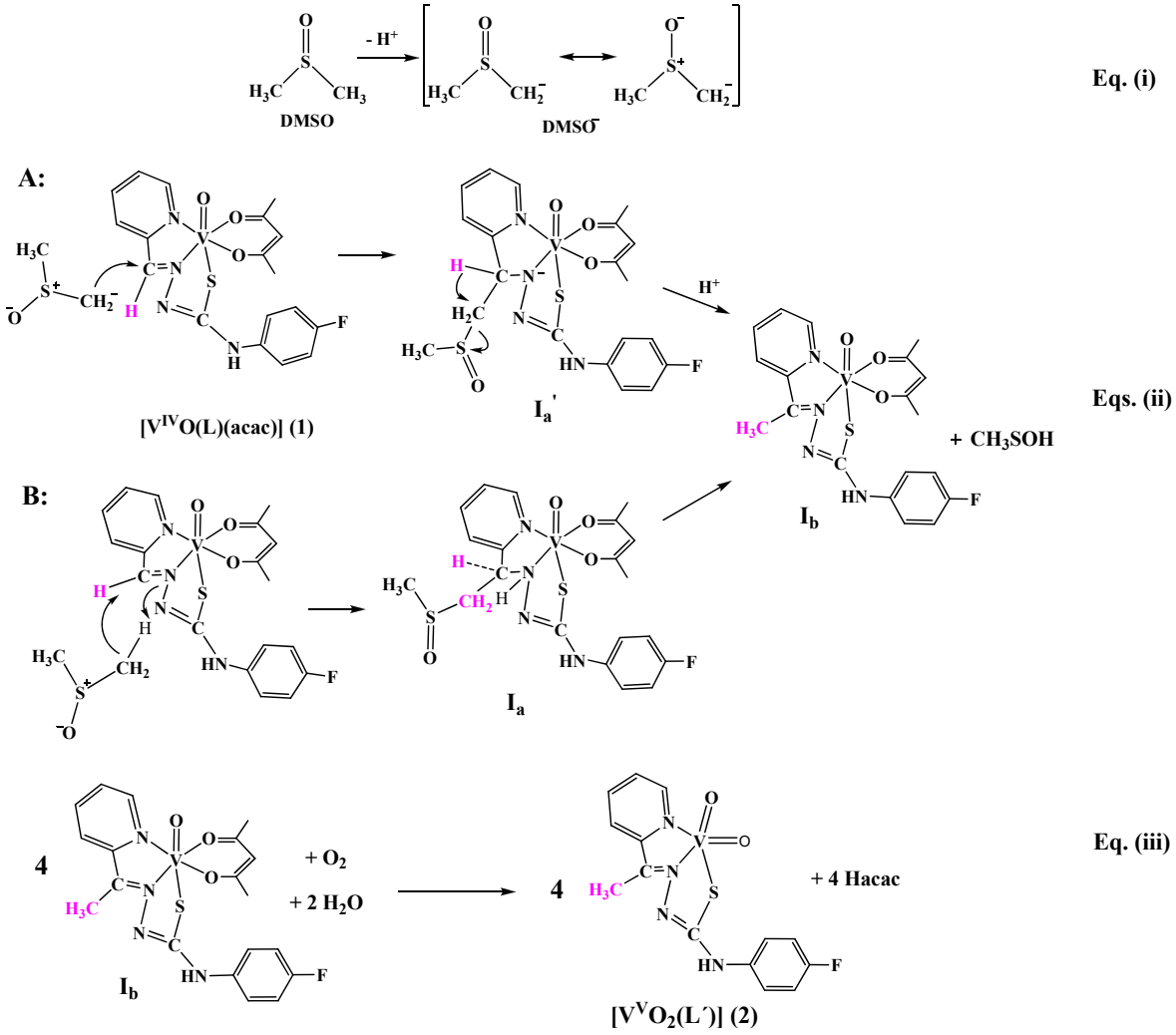

Scheme 2. Processes that are relevant for the formation of $[V^{V}O_2(L')]$ (**2**) from $[V^{IV}O_2(L)(acac)]$ (**1**). Eqs. (ii) correspond to the proposed possible routes A and B for the alkylation of **1** by DMSO at 60 °C.

View Article Online
DOI: 10.1039/C8DT01668B

Pathway A:

A transient nucleophilic dimsyl species might be formed by the loss of one proton from DMSO as depicted in Eq. (i) of Scheme 2. The proton may be taken up by the aldimine N-atom or, in case a transient μ-oxido bridged or hydroxido-$V^{IV}OL$ or $V^{V}OL$ species is formed, the highly basic μ-oxido or hydroxido ligands may bind the proton. The deprotonation of DMSO by either a V-bonded hydroxido or μ-oxido ligand appears also likely, given that the pK_a values of water and DMSO in DMSO are 31.4 and 35.1.[78b-d] In fact, DMSO can be deprotonated by bases weaker than dimsyl such as hydroxide or *t*-butoxide (pK_a of *t*-butanol: 32.2).[78e,f] The deprotonation could also be further facilitated by the increased acidity of the DMSO C-H bonds upon coordination to the oxophilic V^{IV} or V^{V} moieties. Once formed, the dimsyl species attacks the most electrophilic CH moiety nearby (Scheme 2, Eq. ii, A) and forms an intermediate species $\mathbf{I_a}'$, which loses CH_3SOH[78g-i] species to give rise to another intermediate species $\mathbf{I_b}$. Finally, the aerial oxidation of $\mathbf{I_b}$ and loss of a Hacac fragment leads to the formation of $[V^{V}O_2(L')]$ (**2**) (Eq. iii; here the source of the proton might be from the DMSO or the moisture present in the DMSO.)

Pathway B:

This does not require the formation of a dimsyl anion and involves the direct attack of the carbon atom of DMSO to the imine C atom of **1**, (Scheme 2, eq. ii, B) with the formation of the intermediate species **Ia**. This intermediate species then forms CH_3SOH and $\mathbf{I_b}$, which upon oxidation forms **2** (Eq. iii).

The proposed pathways are supported by the Natural Bond Orbital (NBO) atomic charge distribution in complex **1** (Fig. 1a). Among all CH groups, the carbon undergoing methylation has the highest charge together with one of the C atoms of the pyridine ring. There are other C atoms with even higher charges but due to steric and electronic constraints we do not expect there methylation. In addition, the NBO charges at the C atoms of DMSO are strongly negative, particularly in the dimsyl species (Fig. 1b).

View Article Online
DOI: 10.1039/C8DT01668B

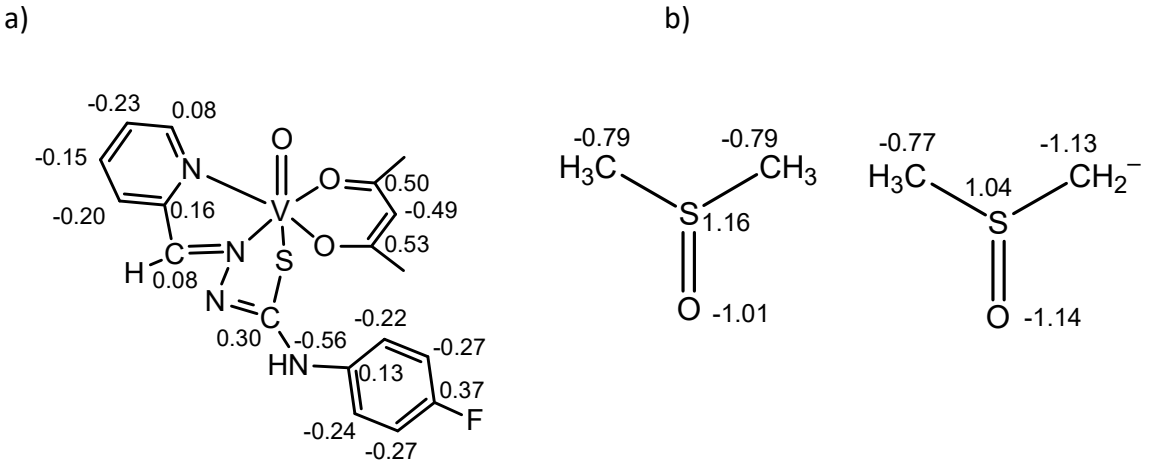

Fig. 1 Diagrams depicting NBO atomic charges at the carbon atoms (a) of **1** and (b) of neutral DMSO (left) and the dimsyl anion (right).

The structures of intermediates $\mathbf{I_a}'$ and $\mathbf{I_a}$ shown in Scheme 2 for pathways A and B were optimized using the DFT (B3P86) method. The addition of the dimsyl anion, $CH_3S(=O)CH_2^-$, to complex **1** giving intermediate $\mathbf{I_a}'$ is highly exoergonic (by –35.3 kcal/mol). In turn, structure $\mathbf{I_a}$ was found to be 0.3 kcal/mol more stable than the initial complex **1** plus DMSO (in terms of ΔG in DMSO solution), which is quite reasonable for a transient reaction species. The free Gibbs energy of the complete reaction (ii) in Scheme 2 (*i.e.*, **1** + DMSO $\rightarrow$ $\mathbf{I_b}$ + CH_3SOH) is –20.7 kcal/mol that indicates the thermodynamic feasibility of this reaction (either pathway A or B). The calculated ΔG_s value of reaction (iii) is –70.2 kcal/mol.

View Article Online
DOI: 10.1039/C8DT01668B

Therefore, both pathways A and B are plausible from the thermodynamic point of view, the relative importance of A and B depending on the temperature, on the pH of the medium and efficacy of basic species (e.g. a μ-oxido or hydroxido vanadium species) in removing a proton from DMSO to yield the $CH_3S(=O)CH_2^-$ anion. Meanwhile, detailed investigation of the mechanistic features and confirmation of the kinetic feasibility of the proposed mechanism should be the subject of a separate work.

IR spectroscopy

The IR spectrum of HL exhibits bands due to ν(N(1)–H) and ν(N(2)–H) moieties in the 3311–2967 cm^{-1} region, but complexes **1**, **2** and **2a** do not exhibit the ν(N(2)–H) band. This indicates that the ligand coordinates to the metal centre in the anionic form. The sharp band at 836 cm^{-1}, due to ν(C(7)–S(1)) stretching in the ligand, is lowered to 775–762 cm^{-1} in the complexes, indicating participation of the thione sulfur in the coordination.[78j,k] Fig. S2 shows the IR spectra of complexes **1** and **2** in the 1100-800 cm^{-1} range. The presence of a strong sharp band at 949 cm^{-1} in **1** suggests the presence of oxido ν(V=O)[79], whereas two peaks in the range 937–922 cm^{-1} in **2** and **2a** are assigned to dioxido (V=O) stretchings.[80] The IR data are summarized in Table 2.

Table 2 IR and electronic spectral data for complexes **1**, **2** and **2a**.

Complex	V–O str,[a] cm^{-1}	UV–Vis[b] λ_{max}, nm (ε, $dm^3mol^{-1}cm^{-1}$)
$[V^{IV}O(L)(acac)]$ (**1**)	949	272 (20703), 332 (25043), 401 (21818), 444 (18182), 603 (120), 761 (45)
$[V^{V}O_2(L')]$ (**2**)	937, 925	<257 (24048), 431 (19919)
$[V^{V}O_2(L)]$ (**2a**)	934, 922	260 (26127), 428 (19919)

[a]In KBr pellet. [b]Solutions in CH_3OH.

View Article Online
DOI: 10.1039/C8DT01668B

UV–Vis spectroscopy

The electronic spectra of **1**, **2** and **2a** were recorded in CH_3OH solution and part of the spectra of complexes **1** and **2** are depicted in Fig. 2. In all complexes two strong absorption bands are observed in the wavelength range 431–257 nm. The lower energy absorptions at 430-400 nm are ascribable to ligand to metal charge transfer (LMCT) transitions,[80a] whereas the higher energy absorptions are likely to be due to ligand centred transitions.[80b] Two weak absorptions at 761 nm (ε_{max} = 45 $dm^3mol^{-1}cm^{-1}$) and 603 nm (ε_{max} = 120 $dm^3mol^{-1}cm^{-1}$) observed for **1** (a V^{IV} complex) are assigned to d–d transitions. [79-81a] The UV–Vis data are summarized in Table 2.

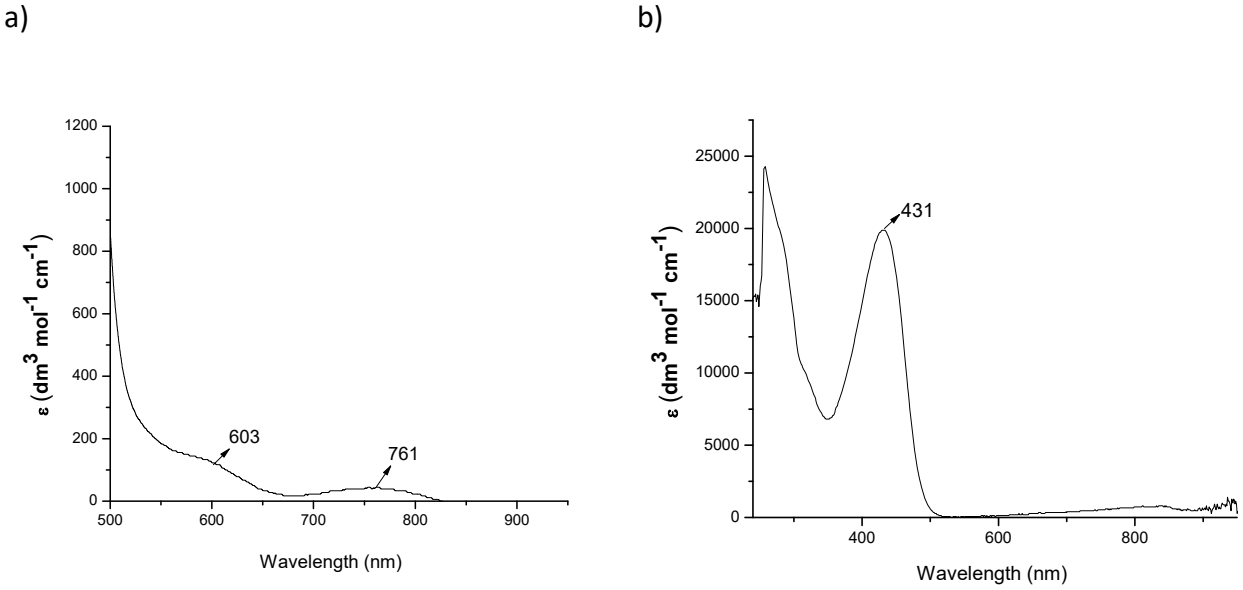

Fig. 2. Part of the electronic absorption spectra of methanolic solutions of (a) [$V^{IV}O(L)(acac)$] (1.8×10^{-4} M) (**1**) and (b) [$V^{V}O_2(L')$] (**2**) (1.5×10^{-5} M).

EPR spectroscopy

The EPR spectrum of **1** was measured in frozen solution of DMF at 77 K (Fig. 3. The spectrum displays a slight rhombicity in the g= 1.95-1.85 region, so it was simulated assuming that the x and y axis are not

View Article Online
DOI: 10.1039/C8DT01668B

equivalent. The experimental spin Hamiltonian parameters obtained are: $g_{x,y}$ =1.977 , $g_{x,y}$ =1.981, g_z=1.95, $|A_{x,y}|$ =51.1 ×10^{-4} cm^{-1}, $|A_{x,y}|$ = 52.6×10^{-4} cm^{-1}, $|A_z|$ = 152.9×10^{-4} cm^{-1}. The obtained *z*-component spin Hamiltonian parameters are consistent with a [N_{im}, N_{py}, O_{acac}, S_{RS}] equatorial donor atom set.[79,81b-e] The $|A_z|$ value calculated by DFT procedures (see above), after the structural optimization of complex **1**, is 154.6×10^{-4} cm^{-1}, reasonably correlating with the experimental value. The DFT calculated $|A_x|$ (58.9×10^{-4} cm^{-1}) and $|A_y|$ (56.2×10^{-4} cm^{-1}) also reasonably agree with the values obtained by simulation of the experimental spectrum.

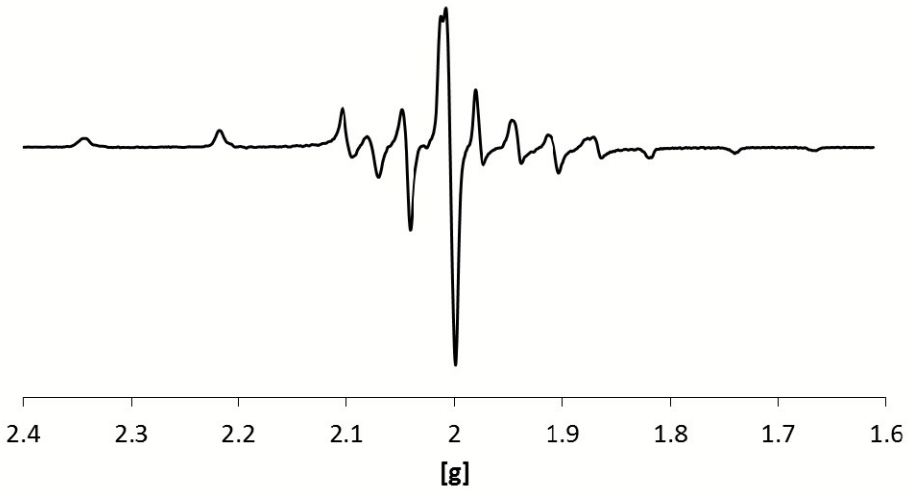

Fig. 3. First derivative of the frozen solution X-Band EPR spectrum of **1** in DMF (0.0025 M) recorded at 77 K.

NMR spectroscopy

The ^{1}H NMR spectrum of HL (Fig. S3) was recorded in DMSO-d_6. It exhibits two singlets in the range 12.08 to 10.29 ppm due to two NH moieties {N(1)H and N(2)H}, whereas in the spectra of complexes **2** and **2a** (Figs. S4 and S5) there is only one peak in the range 10.29 to 10.20 ppm for one NH moiety {N(1)H}, indicating coordination of the ligand to the metal centre in anionic form. The peak due to C(8)H

View Article Online
DOI: 10.1039/C8DT01668B

appears as a singlet at 8.59 ppm for the ligand and at 8.79 ppm for **2a**. The presence of a methyl peak at 2.66 ppm in the spectrum of $[V^{V}O_2(L')]$ (**2**) and absence of a C(8)H peak indicates the methylation at imine carbon C(8) and formation of a new ligand. The detailed NMR data is included in the experimental section.

The reaction of HL with DMSO in the absence and presence of $V^{IV}OSO_4$ or $V^{V}O(OiPr)_3$ was tested further with distinct conditions of temperature and period of reaction, this being monitored by ^{1}H NMR experiments (Figs. S6–S11). No alkylation reaction is noticeable since the CH=N resonance at ca. 8.75 ppm did not subside. These results reinforce the assessment that the methylation reaction may be confined to complex **1**.

Moreover, the reaction of **1** with DMSO at 60°C was monitored by ^{1}H and ^{51}V NMR. A saturated solution of **1** in DMSO was heated to 60°C till all solid dissolved (ca. 10 minutes). A gradual colour change from green to brown was observed. The solution rested at room temperature for another 2 h before NMR analysis. It was observed that the CH=N resonance at *δ* 8.75 ppm nearly disappeared (Figs. 4 and S12).

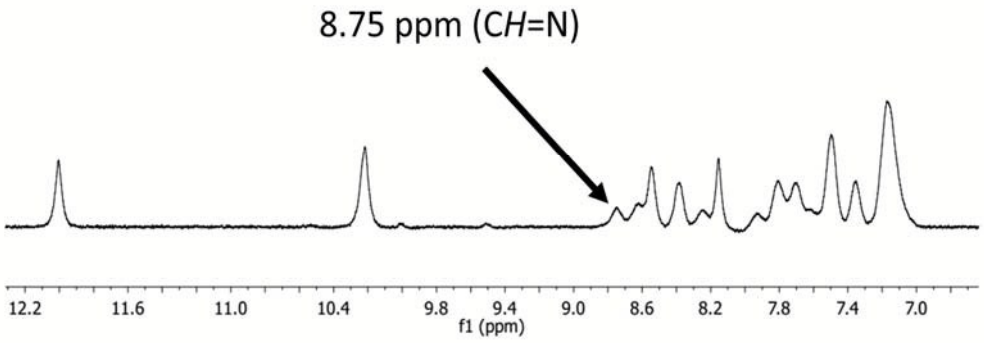

Fig. 4. Low field region of the ^{1}H NMR spectrum of **1** (ca. 0.19 M) in DMSO after heating for 10 min at 60°C and cooling down for 2 h to room temperature. The resonance at 8.75 ppm is assigned to the imine proton (CH=N).

View Article Online
DOI: 10.1039/C8DT01668B

The respective ^{51}V NMR spectrum (Figs. 5 and S13) shows two broad but faint resonances at ca. δ_V = -434 ppm and δ_V = -577 ppm. There are still some $V^{IV}O$-species in solution and the resonances are tentatively assigned to a $V^{V}O_2$-species and a μ-oxido bridged $V^{V}O$-species, respectively. The chemical shift δ_V calculated by DFT (δ_V^{calc}) for **2a** is -433 ppm, thus supporting the assignment of the experimental resonance at -434 ppm; for complex **2** the δ_V^{calc} is -449 ppm. The above observations indicate that the reaction proceeds swiftly at 60 °C.

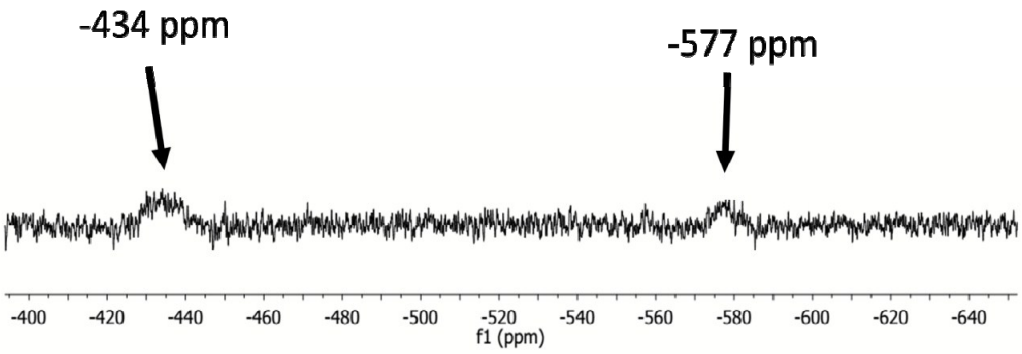

Fig. 5. Close-up of the ^{51}V NMR spectrum of **1** (ca. 0.19 M) in DMSO after heating for 10 min at 60°C and cooling down for 2 h to room temperature.

The reaction of compound **2a** with DMSO at 60 °C was also monitored by ^{1}H and ^{51}V NMR using the same procedure as for **1**. In this case there was no change in color or apparent alteration of the ^{1}H NMR spectrum after 24 h: the CH=N resonance at δ 8.75 ppm remained present with an integration indicative of 1 proton (Fig. S14). Other experiments showed that no alteration occurred after 24 h at 60 °C in DMSO (Fig. S14, B). Only after 5 days under these conditions the CH=N resonance disappeared, but the obtained end product revealed to be a cyclized and oxidized compound **3** (Figs. 9, S1, S15 and S26; see **Table S1** for selected bond lengths and angles). The driving force for this intramolecular cyclisation comes from the highly nucleophilic character of the thiolate moiety. Upon dissociation from the vanadium center, the thiolate attacks the electrophilic imine carbon, forming a cyclic thioaminal. The

View Article Online
DOI: 10.1039/C8DT01668B

aromatisation of this heterocycle to a nitrogenated thiophene favors the subsequent oxidation step, most likely by vanadate(V) formed upon solvolysis of the complex.

The ^{51}V NMR spectrum obtained from the experiments at 24 h showed only one broad but faint resonance at ca. δ_V = -434 ppm, which may be assigned to the *cis*-VO_2 species **2a**. Species at higher field, specifically at δ_V -530 ppm, only appeared after 5 days at 60 ^oC, but by then decomposition of the complex had already occurred. It may be due to an inorganic vanadate species soluble in DMSO, but considering that the ligand undergoes significant transformations it may also be a not characterized and unknown V^V-species. These experiments indicate that the *cis*-dioxidovanadium(V) complex **2a** is unable to mediate the intramolecular methylation of the ligand with DMSO.

NMR spectra upon methylation attempts of other imine ligands

To test the scope of applicability of methylation reactions in DMSO, several other –C=N containing compounds (**L1-L10**) (Chart S1), along with some $V^{IV}O$ complex (for example **C1**, Chart S1), were subjected to the same conditions as those used for **1**. Compounds **L1-L10** were prepared *in situ* by mixing equimolar amounts of an aldehyde or ketone and amine in DMSO. After 5 min of stirring at room temperature, an equimolar amount of $V^{IV}O(acac)_2$ or $V^VO(OiPr)_3$ was added to the reaction mixture. After complete dissolution of the metal precursor the mixture was heated to 60 ^oC in DMSO for 30 min to 1 h, depending on the ligand precursor used. The ^1H NMR spectra of the obtained solutions were measured and compared, when possible, to those obtained for the expected ketimine products (Figs. S16−S22). Somewhat broadened ^1H NMR spectra were obtained in most cases even when a V^V precursor was used. This is due to the significant presence of paramagnetic V^{IV}-species, which in the case of the V^V precursors, could have been formed by the oxidation of the *in situ* ligand. In some instances, such as when **L4** and **L5** were used, significant precipitation of solids precluded the measurement of adequate NMR spectra. Notwithstanding, despite the broadened spectra obtained in most cases, no alkylation

View Article Online
DOI: 10.1039/C8DT01668B

could be detected with any of the compounds **L1-L10** and complexes tested. Importantly, the ligand HL was not alkylated when the metal precursor was $V^{V}O(OiPr)_3$ (Fig. 6). Therefore, these results indicate that the alkylation reaction is confined to the specific case of **1** and, for this system in particular, a $V^{IV}O$-species appears to be a requisite for the reaction to occur.

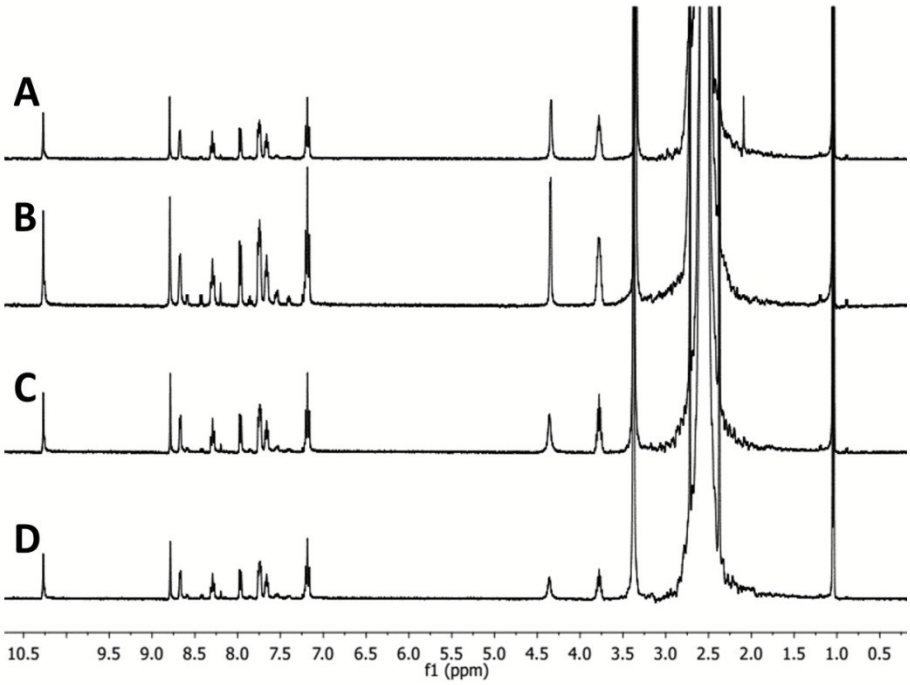

Fig. 6. (A) ^{1}H NMR spectra of a 1:1 mixture of HL and $V^{V}O(OiPr)_3$ in DMSO after 10 min. at 60°C; (B) 1:1 mixture of HL and $V^{V}O(OiPr)_3$ in DMSO after 30 min. at 60°C; (C) 1:1: mixture of HL, $V^{V}O(OiPr)_3$ and H_2O in DMSO after 10 min. at 60°C; (D) 1:1: mixture of HL, $V^{V}O(OiPr)_3$ and H_2O in DMSO after 30 min. at 60°C. No alkylation of HL may be detected from the analysis of these spectra. Reagent concentration was ca. 90 mM.

View Article Online
DOI: 10.1039/C8DT01668B

ESI-MS studies

The negative and positive ESI-MS spectra obtained for compound **1** (Figs. S23 and S24) are of great complexity due to aggregation, but the major peaks were identified. The sample was diluted in methanol in an attempt to minimise aggregation. The observation of methanesulfenic acid or methanesulfenate anion is difficult under the conditions used, given its high reactivity. Instead, we sought to observe methanesulfonic acid (MW = 96.1), as it is the most likely decomposition product of the sulfenic acid. Most of our MS data are for m/z > 100, but nevertheless in the rare ESI-MS spectra recorded with data below m/z of 100, we detected a peak in negative ISI mode at m/z = 95.4 (ca. 85%), (Fig. S25), which may be tentatively attributed to $CH_3SO_3^-$, which might have resulted from the CH_3SOH formed (eq. (ii) in Scheme 2).

The ESI-MS spectrum in the negative mode shows two identifiable major species at m/z = 355 and 385 which are assigned respectively to the free methylated ligand (HMeL) $[(MeL)\cdot 2H_2O\cdot MeOH]^-$ (m/z= 355) and the complex $\{[V^{IV}O(MeL)]OMe\}^-$(m/z=385). As for the positive mode ESI-MS spectrum, three major peaks were identified: (1) the peak at m/z = 242 is assigned to $\{[V^{IV}O(HMeL)]\cdot 4MeOH\}^{2+}$ (m/z= 483/2 = 241.5), whereas (2) the peak at m/z = 321 is assigned to $[(H_2MeL)\cdot MeOH]^+$, and (3) the peak at m/z = 778 is tentatively assigned to a mixed valence μ-oxido bridged species, $\{Na[V^{V}O(MeL)OMe]\mu\text{-}O[V^{IV}O(MeL)]\}^+$. Lower mass peaks are present in both positive and negative spectra, which are indicative of fragmentation. In the positive mode the weak peak at 439.97 could be assigned to the molecular ion $\mathbf{1}\cdot H^+$. Despite the complexity of the obtained MS spectra, these clearly show that a reaction between **1** and DMSO took place with the formation of methylated products.

Electrochemical properties

The electrochemical properties of **1** and **2** were examined in CH_3CN solution (0.1 M TEAP) by cyclic voltammetry using a platinum working electrode, platinum auxiliary electrode, and Ag/AgCl reference

View Article Online
DOI: 10.1039/C8DT01668B

electrode. The potential data are listed in Table 3. The voltammogram pattern for **1** includes both oxidation and reduction processes (Fig. 7(a)); the redox couple at $E_{1/2}$ value 0.62 V corresponds to V^{IV}/V^{V} oxidation, whereas $E_{1/2}$ at –1.13 V corresponds to V^{IV}/V^{III} reduction couple. The voltammogram pattern for **2** includes only a quasi-reversible redox couple at $E_{1/2}$ = –0.73 V corresponding to V^{V}/V^{IV} reduction (Fig. 7(b)). The redox characteristics of **2a** were also examined by measuring the corresponding voltammogram; as expected it is very similar to that of complex **2**.

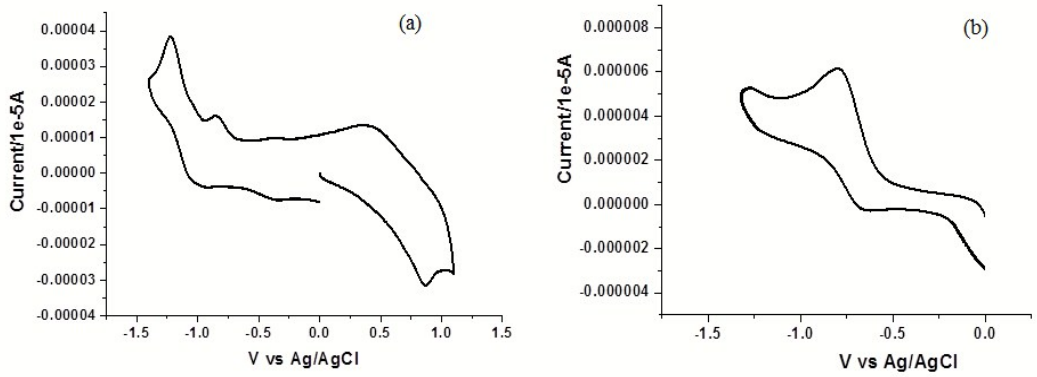

Fig. 7. Cyclic voltammograms of $[V^{IV}O(L)(acac)]$ (**1**) (a) and $[V^{V}O_2(L')]$ (**2**) (b) in CH_3CN solution.

Table 3 Cyclic voltammetric[a] data for $[V^{IV}O(L)(acac)]$ (**1**) and $[V^{V}O_2(L')]$ (**2**) at 298 K.

Complex	V^{IV}/V^{V}	V^{IV}/V^{III}	V^{V}/V^{IV}
	$E^{a}_{1/2}$ (V), ΔE^{a}_{P} (mV)	$E^{c}_{1/2}$ (V), ΔE^{c}_{P}(mV)	$E^{c}_{1/2}$ (V), ΔE^{c}_{P} (mV)
$[V^{IV}O(L)(acac)]$ (**1**)	0.62, 450	–1.13,200	–
$[V^{V}O_2(L')]$ (**2**)	–	–	–0.73, 120

[a]In CH_3CN at a scan rate 100 mV/s. $E_{1/2} = (E_{pa} + E_{pc})/2$, where E_{pa} and E_{pc} are anodic and cathodic peak potentials vs. Ag/AgCl, respectively. $\Delta E_P = E_{pa} - E_{pc.}$

View Article Online
DOI: 10.1039/C8DT01668B

X-ray diffraction crystallography.

It was not possible to obtain X-ray diffraction crystals of **1** with adequate quality but, there are two closely related structures in the literature. These feature very similar atom donor sets, geometries and with oxido and $acac^-$ ligands as in **1** but, with 2-acetylpyridine-4-phenylthiosemicarbazato[82] and dimethylthiosemicarbazonato[83] as the tridentate ligands.

A view of the molecular structure of **2** is shown in Fig. 8 and selected geometric parameters are collected in Table 4. In this structure, the V(V) atom is bonded to the S, N, N-donors of the uninegative tridentate ligand, as for **1**, and two oxido-O atoms. The length of the C–S bond [1.730(3) Å] is suggestive that the ligand is coordinating as a thiolate, a conclusion also supported by the short C7–N2 [1.305(4) Å] and C8–N3 [1.306(4)] bonds. The V1,S1,N2,N3,C7 and V,N3,N4,C8,C10 five-membered chelate rings are each planar, having r.m.s. deviations of 0.018 and 0.015 Å, respectively, and form a dihedral angle of 2.6(1)°. The pyridyl ring forms dihedral angles of 4.26(17) and 4.0(5)° with the adjacent chelate ring and terminal fluorophenyl ring, respectively, indicating that the entire tridentate ligand is approximately planar. The N_2O_2S donor set defines a highly distorted coordination geometry as seen in the value of the trigonality index, τ = 0.43, which is intermediate between square pyramidal (τ = 0.0) and trigonal bipyramidal (τ = 1.0).[84] To a first approximation, the observed molecular structure of **2** matches that reported for the *N*-bound methyl derivative which differs in geometric parameters. In the latter the V–S [2.3759(9) Å], V–O [1.631(2) Å] and N3–C8 [1.323(4) Å] bond lengths are marginally longer than in **2**;[28] the coordination geometry is closer to square pyramidal (τ = 0.22).

View Article Online
DOI: 10.1039/C8DT01668B

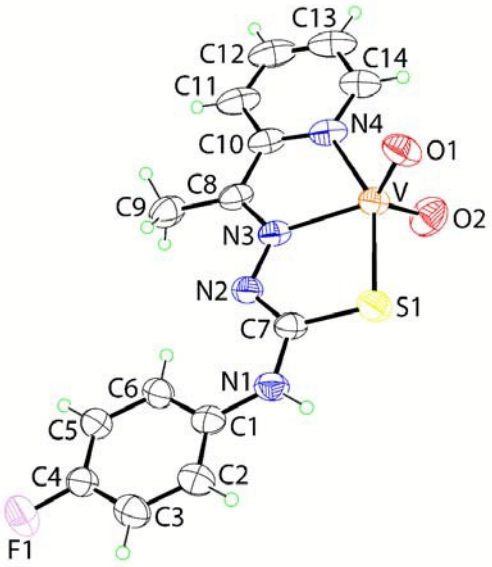

Fig. 8. Ortep representation (35%) showing a view of the molecular structure of **2**; one of the disorder components of the fluorophenyl ring was omitted for reasons of clarity.

Table 4 Selected geometric parameters (Å, °) for **2**

Atoms	Parameter	Atoms	Parameter
Complex **2**			
V–S1	2.3653(13)	V–O1	1.607(2)
V–O2	1.596(3)	V–N3	2.143(3)
V–N4	2.086(3)	C7–S1	1.730(3)
C7–N2	1.305(4)	N2–N3	1.374(4)
C8–N3	1.306(4)		
S1–V–O1	101.93(10)	S1–V–O2	98.93(11)
S1–V–N4	77.58(7)	S1–V–N4	151.34(10)
O1–V–O2	110.14(16)		

View Article Online
DOI: 10.1039/C8DT01668B

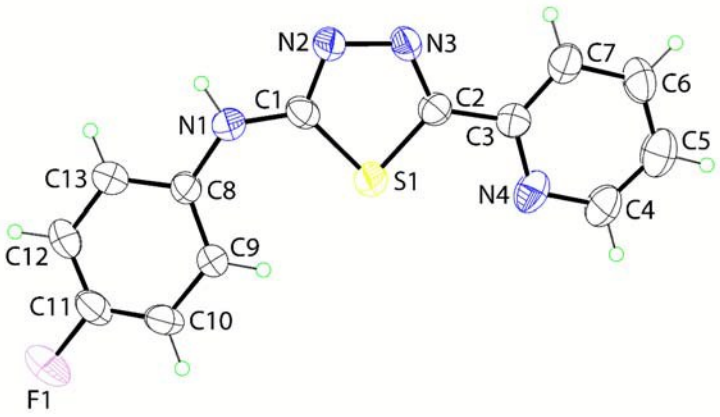

Fig. 9. Ortep representation (35%) showing a view of the molecular structure of **3**, first independent molecule.

Two independent molecules comprise the asymmetric unit of **3**, Figs. 9 and S26 (a), and these adopt very similar conformations as seen in the overlay diagram in Fig. S26 (b). The structure features a 1,3,4-thiadiazolyl ring with 4-fluorophenylamine and 2-pyridyl substituents at the 2- and 5-positions. The molecular packing of compounds **2** and **3** are discussed in the ESI section (Figs. S26-S29).

***In vitro* insulin-like activity. *In* vitro insulin mimetic activity.** Vanadium compounds are known to have insulin enhancing effect[17,19,30,32,33,36,37,41,42a,b,d,43a,c] both *in vitro* and *in vivo.* In this study [$V^{IV}O$(L)(acac)] (**1**) and [$V^{V}O_2$(L´)] (**2**) were tested for this feature in an *in vitro* glucose uptake assay. In L6 myotubes, a cell line of skeletal muscle origin, glucose uptake in response to insulin stimulation plays a key role in the whole body glucose homeostasis. Glucose transporter GLUT4 is the major glucose transporter of muscle exquisitely regulated by insulin through posttranslational events.[85] The L6 myotubes differentiated from L6 myoblast have the ability to respond to insulin via insulin receptor signaling and translocation of GLUT4 to the plasma membrane. The hyperglycemic condition was created in cell culture by incubating the cells in 25 mM glucose. Complex **1** at 100 µM concentration showed glucose uptake stimulating activity in the myotubes which was found to be comparable to that of 2 µM of insulin (Fig. 10). Complex **2** at 100 µM concentration also showed considerable insulin-like activity, whereas in the conditions of our experiments $V^{IV}O(acac)_2$ showed negligible insulin enhancing effects at the concentrations tested. In

View Article Online
DOI: 10.1039/C8DT01668B

case of **1**, the enhancement of the insulin mimetic activity, with respect to **2**, might be related to the difference in the oxidation state of the complexes as vanadium(IV) complexes; similar differences between the effects of V^{IV}- and V^{V}-compounds has been often mentioned.[86] Noteworthy is the observation that in our *in vitro* data both **1** and **2** have significantly higher insulin-like activity than $V^{IV}O(acac)_2$, a compound previously shown to be insulin enhancing both *in vitro* and *in vivo*.[34,35]

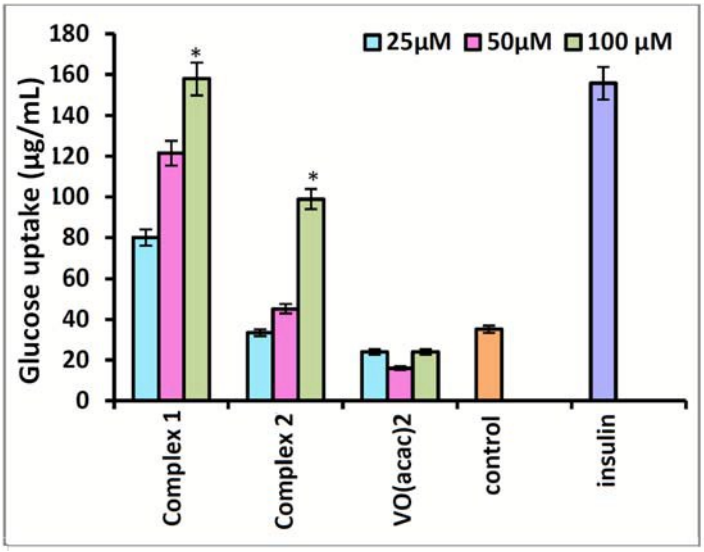

Fig. 10. Effect of complexes (**1** and **2**) on glucose uptake in cultured L6 myotubes under high glucose conditions (25 mM Glucose). Three concentrations 25 µM, 50 µM and 100 µM were tested for each complex. The data is indicated as mean ± SEM (n=3). Student's t–Test was used where bars with asterisk show a significant difference (*P< .05) with respect to the untreated control.

Cytotoxicity Studies. Vanadium compounds have increasingly being considered to have potential as anti-cancer drugs,[19,20,21b] so to evaluate the potentiality of these compounds as drugs for the treatment of cancer, in the present work *in vitro* cytotoxicity studies of complexes **1** and **2** was assayed by determining the viability of MCF–7 (breast cancer cells) and Vero cells (noncancerous mammalian cells) using the MTT assay. The ligand HL and $V^{IV}O(acac)_2$ gave high IC_{50} values at 24 h higher than 200 µM, whereas $[V^{IV}O(L)(acac)]$ (**1**) and $[V^{V}O_2(L')]$ (**2**) gave lower IC_{50} values that are depicted in Table 5. It was

View Article Online
DOI: 10.1039/C8DT01668B

observed that, upon increase in time of incubation from 24 to 72 h, the IC_{50} values decrease, being lower for the Vero cells, but they do not differ much for 48 and 72 h. In comparison to the IC_{50} values obtained, cisplatin a well-established chemotherapeutic drug, has an IC_{50} value of 28±6 μM at 72 h.[87] The cytotoxicity of some $V^{IV}O$-complexes of salicylaldimines and polypyridyl ligands, here designated as [$V^{IV}O$(sal-AMA)(NN)] were recently also studied against MCF-7 cells,[87] where the IC_{50} values varied between 5.9 ± 1.4 to 40.9 ± 7.5 μM at 24 h and between 2.8 ± 1.3 to 8.4 ± 2.4 μM at 72 h. The present compounds depict comparable IC_{50} values at 24 h to those of this previous report, but with somewhat higher IC_{50} values; thus complexes **1** and **2** are less toxic against MCF-7 cells than the tested [$V^{IV}O$(sal-AMA)(NN)] compounds.[87] Noteworthy, **1** and **2** are more toxic for the Vero cells, used here as reference for normal cells, thus their selectivity does not appear adequate, at least when solely compared against this cell line.

Table 5 IC_{50} (μM) values in MCF–7 and Vero cell lines for complexes 1 and 2

Cell Line	Time / h	IC_{50} values (μM)	
		1	**2**
MCF-7	24	28.5 ± 0.45	115.6 ±1.02
	48	26.3 ± 0.36	90.6 ±0.97
	72	23.2 ± 0.38	84.0 ±0.93
Vero cells	24	41.6 ± 0.54	120.6 ± 1.12
	48	3.1 ±0.25	30.1 ± 0.31
	72	3.2 ±0.28	29.4 ±0.38

View Article Online
DOI: 10.1039/C8DT01668B

The higher IC_{50} values of HL (and of $V^{IV}O(acac)_2$) in comparison to the metal complexes **1** and **2** indicate that the incorporation of vanadium in the ligand environment increases the cytotoxicity towards these cells. It is plausible that the permeation of the vanadium complexes through the lipid layer of the cell membrane is favoured by coordination, the polarity of the ligand and the central metal ion being globally decreased through charge equilibration.[88,34a] Bovine serum albumin (BSA) is present in relatively high concentration in FBS, which was added in 10% to the incubation medium. Albumins, e.g. BSA may serve as vehicles of uptake of drugs, namely metal-based drugs[34b] by the cells, thus it is also possible that the higher toxicity of **1** and **2** when compared to the ligand, might be due to distinct binding to the albumin leading to a more efficient uptake in the case of complexes **1** and **2**. Similarly with $V^{IV}O(acac)_2$ which binds albumins rather weakly.[35]

It may be concluded from the present *in vitro* data that the metal complexes exhibit greater biological activities than the free ligands, which is also in accordance with previous reports.[89,90] Apart from the possible higher uptake of complexes when compared with the corresponding ligands, or synergistic effects operating, vanadium ions by themselves present some toxicity.[91] Comparing the activity of the two complexes, it is observed that the toxicity of $[V^{IV}O(L)(acac)]$ (**1**) is greater than that of $[V^{V}O_2(L')]$ (**2**), which is reflected from their IC_{50} values with dose dependency illustrated in Fig. 11 and Table 5, which can either be correlated with the difference in the oxidation states of the complexes and/or to different uptake efficiency by the cells.

View Article Online
DOI: 10.1039/C8DT01668B

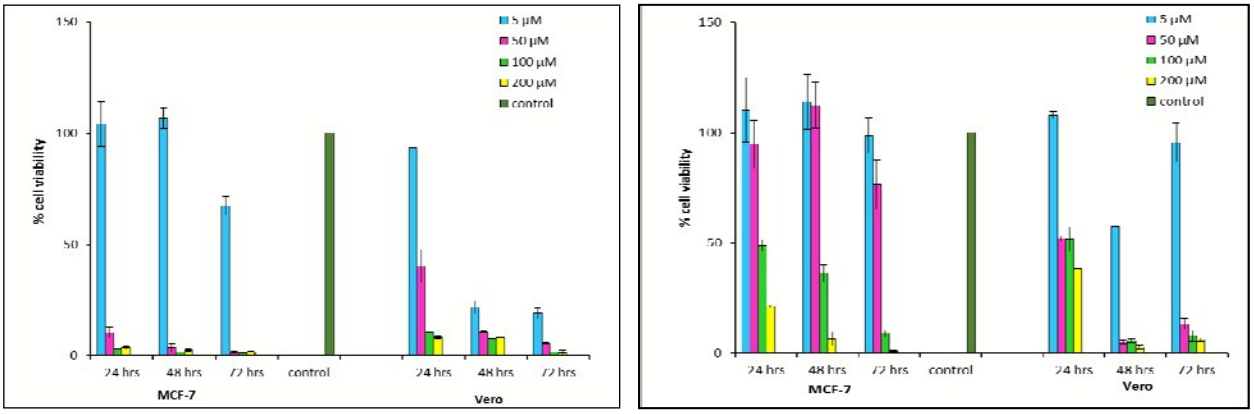

Fig. 11 Effect of [$V^{IV}O(L)(acac)$] (**1**) (a) and [$V^{V}O_2(L')$] (**2**) (b) on cell viability and growth: MCF–7 and Vero cells were treated with different concentrations of the test compound for 24 h, 48 h and 72 h and then cell viability was measured by the MTT assay. Data reported as the mean ± S.D. for *n* = 3 and compared against control (considered as 100% viability).

Nuclear staining assay. Aspects of the mechanism of cell death due to the complexes (**1** and **2**) were checked by staining dying cells with DAPI. The density of the DAPI stained nuclei was used to check the dead cells or those that have compromised membranes in different treatment groups. Fig. 12 shows images taken after DAPI staining in blue fluorescence at different concentrations of the complexes. It can be seen from the figure that the number of DAPI stained nuclei were reduced in treated wells with increasing concentrations of the complexes indicating the dose dependent cell death. Fig. 13 shows the grey scale images at different time points after the treatment with minimum toxic concentrations of the complexes (5 µM). The distinct nuclear condensation and fragmentation was seen in treated cells compared to control cells. Upon increase in time of incubation (from 24−72 h), the treated cells exhibited a shrinking morphology which indicated that, with increase in time, apoptosis of the cells took

View Article Online
DOI: 10.1039/C8DT01668B

place. The changes with increasing of incubation time were more drastic for complex **2** which is significantly more cytotoxic than complex **1**.

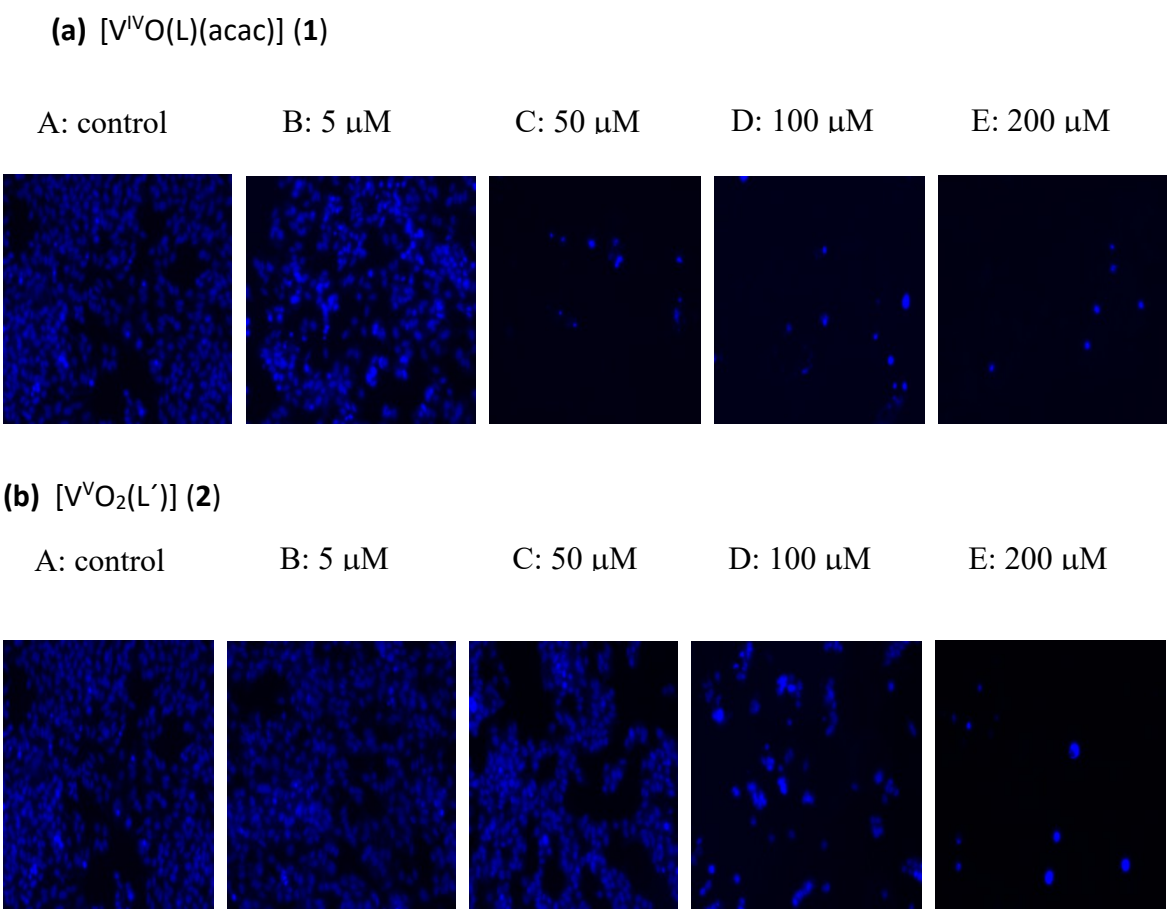

Fig. 12. Changes of MCF-7 cells observed by fluorescence microscopy upon staining with DAPI (see experimental) after 24 h incubation. Images B–E clearly show the decrease in the number of live cells with increasing concentration of the drugs (compared to the control, A).

View Article Online
DOI: 10.1039/C8DT01668B

(a) [$V^{IV}O(L)(acac)$] (**1**):

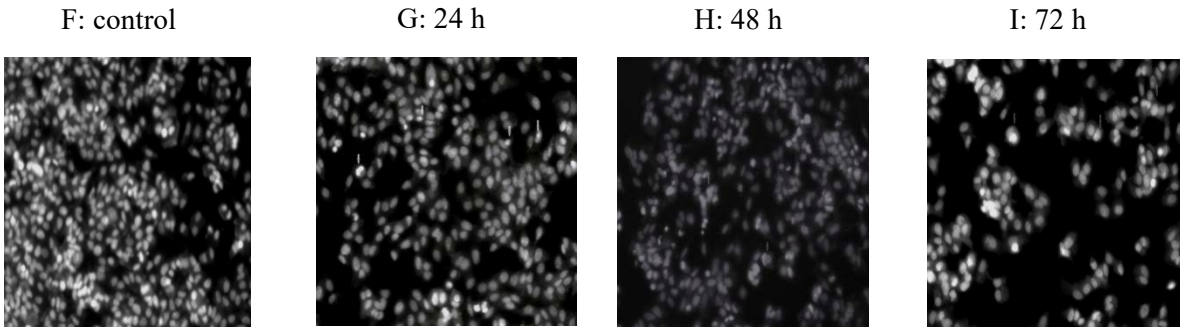

(b) [$V^{V}O_2(L')$] (**2**):

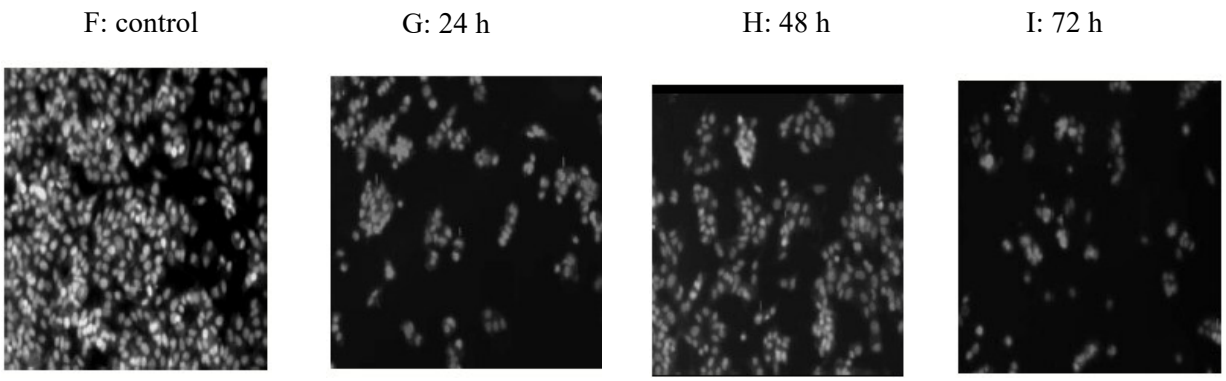

Fig. 13 (a and b). Changes of MCF-7 cells observed by fluorescence microscopy upon staining with DAPI: F-I show changes in nuclei with respect to the treatment time. Arrows show the morphological changes in nuclei of MCF-7 cells observed on applying 5 μM vanadium complexes (**1** and **2**) in comparison to control.

View Article Online
DOI: 10.1039/C8DT01668B

Conclusions

The syntheses and characterization of the $V^{IV}O$-complex $[V^{IV}O(L)(acac)]$ (**1**) and of two $V^{V}O_2$-complexes $[V^{V}O_2(L')]$ (**2**) and $[V^{V}O_2(L)]$ (**2a**), prepared with the Schiff based derived from 4-(*p*-fluorophenyl) thiosemicarbazone and pyridine-2-aldehyde (HL) is achieved. The synthesized HL and the metal complexes were characterized by elemental analysis and spectroscopic studies.

Complex $[V^{IV}O(L)(acac)]$ (**1**) is found to undergo methylation at the aldimine carbon of the ligand in the presence of DMSO forming the $V^{V}O_2$-species $[V^{V}O_2(L')]$ (**2**), which was also characterized by single crystal X-ray diffraction. A nucleophilic dimsyl species ($CH_3SOCH_2^-$), generated from DMSO, or direct attack of the CH_3SOCH_3 carbon to the aldimine carbon, is probably responsible for the methylation reaction. In attempts to carry out similar methylation under similar reaction conditions with various other ligands and complexes prepared from different vanadium precursors or when using the $V^{V}O_2$-complex **2a**, or ligand L in the presence of $V^{V}O(OiPr)_3$, were not successful. Hence, it can be concluded that the methylation of the aldimine carbon by DMSO only takes place with **1**, is ligand specific and takes place only when vanadium is in $V^{IV}O$ state. Keeping **2a** dissolved in DMSO at ca. 60 ^{o}C, within a few hours the thiolate attacks the electrophilic imine carbon, forming a cyclic thioaminal **3**. Thus, instead of methylation after 5 days a cyclised and oxidised compound was isolated.

Complexes **1** and **2** show *in vitro* insulin mimetic activity against insulin responsive L6 myoblast cells, both being more active than $V^{IV}O(acac)_2$. The *in vitro* cytotoxicity studies of complexes **1** and **2** against the MCF–7 and Vero cell lines showed that the compounds are not very toxic. DAPI staining experiments revealed that, upon increase in time of incubation, shrinking morphology of the cells were observed, which is an important hallmark of apoptosis.

View Article Online
DOI: 10.1039/C8DT01668B

Conflicts of interest

There are no conflicts of interest to declare.

Acknowledgements

The authors thank the reviewers for their comments and suggestions, which were helpful in preparing the revised version of the manuscript. Financial support by DAAD (short term research stay during May-June, 2017 of R.D. at FSU, Jena, Germany) is acknowledged. R.D. thanks Dr. Bimba N. Joshi for biological study and discussion. The authors thank DBT, Govt. of India [Grant No. 6241 P112/RGCB/PMD/DBT/RPDA/2015] for funding this research. Financial support by FCT-Fundação para a Ciência e Tecnologia (projects UID/QUI/00100/2013, RECI/QEQ-QIN/0189/2012 and RECI/QEQ-MED/0330/2012), and grants SFRH/BPD/79778/2011 and SAICT nº 22125) and the Portuguese NMR and Mass Spectrometry IST-UL Nodes are acknowledged. The X-ray crystallography laboratory at the University of Malaya is thanked for providing the X-ray data for **2**.

Notes and references

Corresponding Author

*E-mail: rupamdinda@nitrkl.ac.in (R. Dinda)

*E-mail: joao.pessoa@ist.utl.pt (João Costa Pessoa)

†Electronic supplementary information (ESI) available (Table S1, Figs S1−S29): CCDC reference numbers 1825055 (compound **2**) and 1825053 (compound **3**). For ESI and crystallographic data in CIF format see DOI: XXXXX

View Article Online
DOI: 10.1039/C8DT01668B

References:

(1) (a) G. A. Russel and S. A. Weiner, *J. Org. Chem.*, 1966, **31**, 248-251; (b) X. Jiang, C Wang, Y. Wei, D. Xue, Z. Liu and J. Xiao, *Chem. Eur. J.*, 2014, 58-63; (c) B. N. Atkinson and J. M. J. Williams, *Chem Cat Chem*, 2014, 1860-1862; (d) R. Oda and Y. *Hayashi, Bull. Inst. Chem. Res. Kyoto Univ*., 1970, **47**, 480-521; (e) M. K. Eberhardt and R. Colina, *J. Org. Chem.* 1988, **53**, 1071-1074.

(2) *Vanadium Compounds, Chemistry, Biochemistry and Therapeutic Applications* (Eds.: Tracey, A. S.; Crans, D. C.), ACS Symp. Ser. **711**, 1998.

(3) *Vanadium and Its Role in Life* (vol. **31** of *Metal Ions in Biological Systems*; Eds: Sigel, H.; Sigel, A.), Marcel Dekker, New York, 1995.

(4) D. Rehder, *Coord. Chem. Rev.*, 1999, **182**, 297-322.

(5) *Vanadium in the Environment* (Ed.: Nriagu, J. O.), Wiley, New York, 1998.

(6) A. Tracey, G. R. Willsky and E. S. Takeuchi, *Vanadium. Chemistry, Biochemistry, Pharmacology and Practical Applications*, CRC Press, Boca Raton, 2007.

(7) J. C. Pessoa, E. Garribba, M. F. A. Santos and T. Santos-Silva, *Vanadium and proteins: uptake, transport, structure, activity and function*, *Coord. Chem. Rev*., 2015, **301**–**302,** 49-86.

(8) D. Rehder, *The future for vanadium, Dalton Trans*., 2013, **42**, 11749-11761.

(9) D. C. Crans, J. J. Smee, E. Gaidamauskas and L. Yang, *The Chemistry and Biochemistry of Vanadium and the Biological Activities Exerted by Vanadium Compounds. Chem. Rev.,* 2004, **104**, 849-902.

(10) T. Hirao, *Chem. Rev.,* 1997, **97**, 2707-2724.

(11) I. W. C. E. Arends, M. Pellizon and R. A. Sheldon, *Stud. Surf. Sci. Catal.,* 1997, **110**, 1031-1040.

(12) M. Sutradhar, L. M. D. R. S. Martins, M. F. C. G. da Silva and A. J. L. Pombeiro, *Vanadium complexes: Recent progress in oxidation catalysis. Coord. Chem. Rev.*, 2015, **301**, 200-239.

(13) J. A. L. da Silva, J. J. R. F. da Silva and A. J. L. Pombeiro, *Oxovanadium complexes in catalytic oxidations. Coord. Chem. Rev.*, 2011, **255**, 2232-2248.

(14) V. Conte, A. Coletti, B. Floris, G. Licini and C. Zonta, *Mechanistic aspects of vanadium catalysed oxidations with peroxides. Coord. Chem. Rev.*, 2011, **255**, 2165-2177.

View Article Online
DOI: 10.1039/C8DT01668B

(15) M. R. Maurya, A. Kumar and J. C. Pessoa, *Vanadium complexes immobilized on solid supports and their use as catalysts for oxidation and functionalization of alkanes and alkenes. Coord. Chem. Rev.*, 2011, **255**, 2315-2344.

(16) M. Kirihara, *Aerobic oxidation of organic compounds catalyzed by vanadium compounds. Coord. Chem. Rev.*, 2011, **255**, 2281-2302.

(17) K. H. Thompson, J. H. McNeill and C. Orvig, *Chem. Rev.,* 1999, **99**, 2561-2572.

(18) T. Jakusch and T. Kiss, *Coord. Chem. Rev.,* 2017, **351**, 118-126.

(19) J. C. Pessoa, S. Etcheverry and D. Gambino, *Vanadium compounds in medicine. Coord. Chem. Rev*., 2015, **301**, 24-48.

(20) E. Kioseoglou, S. Petanidis, C. Gabriel and A. Salifoglou, *The chemistry and biology of vanadium compounds in cancer therapeutics. Coord. Chem. Rev*., 2015, **301**, 87-105.

(21) (a) D. Gambino, *Potentiality of vanadium compounds as anti-parasitic agents. Coord. Chem. Rev*., 2011, **255**, 2193-2203; (b) M. Selman et al., *Multi-modal Potentiation of Oncolytic Virotherapy by Vanadium Compounds, Mol. Ther.*, 2018, **26**, 56-69.

(22) M. J. Xie, Y. F. Niu, X. D. Yang, W. P. Liu, L. Li, L. H. Gao, S. P. Yan and Z. H. Meng, *Eur. J. Med. Chem.*, 2010, **45**, 6077-6084.

(23) I. C. Mendes, L. M. Botion and A. V. M. Ferreira, *Inorg. Chim. Acta*, 2009, **362**, 414-420.

(24) J. Benítez, L. Guggeri, I. Tomaz, J. C. Pesso, V. Moreno, J. Lorenzo, F. X. Avilés, B. Garat and D. Gambino, *J. Inorg. Biochem.*, 2009, **103**, 1386-1394.

(25) J. Lu, H. Guo, X. Zeng, Y. Zhang, P. Zhao, J. Jiang and L. Zang, *J. Inorg. Biochem*., 2012, **112**, 39-48.

(26) I. Correia, P. Adao, S. Roy, M. Wahba, C. Matos, M. R. Maurya, F. Marques, F. R. Pavan, C. Q. F. Leite, F. Avecilla and J. C. Pessoa, *Hydroxyquinoline derived vanadium(IV and V) and copper(II) complexes as potential anti-tuberculosis and anti-tumor agents. J. Inorg. Biochem.,* 2014, **141**, 83-93.

(27) J. Benítez, L. Becco, I. Correia, S. M. Leal, H. Guiset, J. C. Pessoa, S. Tanco, P. Escobar, V. Moreno, B. Garat and D. Gambino, *J. Inorg. Biochem.*, 2011, **105**, 303-312.

(28) P. I. da S. Maia, F. R. Pavan, C. Q. F. Leite, S. S. Lemos, G. F. de Sousa, A. A. Batista, O. R. Nascimento, J. Ellena, E. E. Castellano, E. Niquetf and V. M. Deflon, *Polyhedron*, 2009, **28**, 398-406.

View Article Online
DOI: 10.1039/C8DT01668B

(29) (a) Y. Wei, C. Zhang, P. Zhao, X. Yang and K. Wang, *J. Inorg. Biochem*., 2011, **105**, 1081-1085; (b) M. Sutradhar, T. R. Barman, G. Mukherjee, M. Kar, S. S. Saha, M. G. B. Drew and S. Ghosh, *Inorg. Chim. Acta,* 2011, **368**, 13-20; (c) A. R. Saltiel and C. R. Khan, *Nature,* 2001, **414**, 799-806; (d) P. Noblía, E. J. Baran, L. Otero and D. Gambino, *Eur. J. Inorg. Chem*., 2004, 322-328; (e) J. Nilsson, A. A. Shteinman, D. Rehder and E. Nordlander, *J. Inorg. Biochem.*, 2011, **105**, 1795-1800; (f) G. R. Willsky, L.-H. Chi, Z. Hu and D. C. Crans, *Coord. Chem. Rev.*, 2011, **255**, 2258-2269; (g) D. Rehder, *Inorg. Chem. Commun*., 2003, **6**, 604-617; (h) M. N. Islam, A. A. Kumbhar, A. S. Kumbhar and B. N. Joshi, *Inorg. Chem.*, 2010, **49**, 8237-8246; (i) S. I. Pillai, S. P. Subramanian and M. Kandaswamy, *Eur. J. Med. Chem*., 2013, **63**, 109-117.

(30) K. H. Thompson and C. Orvig, *J. Chem. Soc. Dalton Trans*., 2000, 2885-2892.

(31) D. Rehder, J. C. Pessoa, C. F. G. C. Geraldes, M. M. C. A. Castro, T. Kabanos, T. Kiss, B. Meier, G. Micera, L. Pettersson, M. Rangel, A. Salifoglou, I. Turel and D. Wang*, "In vitro study of the insulin-mimetic behaviour of vanadium(IV, V) co-ordination compounds", J. Biol. Inorg. Chem.,* 2002, **7**, 384-396.

(32) K. H. Thompson, J. Lichter, C. Lebel, M. C. Scaife, J. H. McNeill and C. Orvig, *Vanadium treatment of type 2 diabetes: A view to the future. J. Inorg. Biochem.*, 2009, **103**, 554-558.

(33) H. Sakurai, Y. Yojima, Y. Yoshikawa, K. Kawabe and H. Yasui, *Antidiabetic vanadium(IV) and zinc(II) complexes. Coord. Chem. Rev.,* 2002, **226**, 187-198.

(34) (a) Y. Shechter and S. J. D. Karlish, *Nature,* 1980, **284**, 556–558; (b) C. E. Heyliger, A. G. Tahiliani and J. H. McNeill, *Science,* 1985, **227**, 1474-1477.

(35) S. Ramanadham, J. J. Mongold, R. W. Brownsey, G. H. Cros and J. H. McNeill, *Am. J. Physiol.,*1989, **257**, 904-911.

(36) J. H. McNeill, V. G. Yuen, H. R. Hoveyda and C. Orvig, *J. Med. Chem.,* 1992, **35**, 1489-1491.

(37) T. Storr, K. H. Thompson and C. Orvig, *Chem. Soc. Rev.*, 2006, **35**, 534-544.

(38) Y. Schecter, J. Meyerovitch, Z. Farfel, J. Sack, S. Bar-Meir, S. Amir, H. Degani and S. J. D. Karlish, *Vanadium in Biological Systems; Kluwer Academic Publishers: Norwell, MA*, 1990; pp 129.

(39) K. H. Thompson, J. H. McNeill and C. Orvig, *Topics in Biological Chemistry: Metallopharmaceuticals; Springer-Verlag: Heidelberg,* 1999; Vol. 31, pp 139.

View Article Online
DOI: 10.1039/C8DT01668B

(40) A. Levina, A. I. McLeod, L. E. Kremer, J. B. Aitken, C. J. Glover, B. Johannessen and P. A. Lay, *Reactivity-activity relationships of oral antidiabetic vanadium complexes in gastrointestinal media: an X-ray absorption spectroscopic study. Metallomics*, 2014, **6**, 1880-1888.

(41) K. H. Thompson and C. Orvig, *J. Inorg. Biochem.,* 2006, **100**, 1925-1935.

(42) (a) H. Sakurai, J. Fugono and H. Yasui, *Mini-Rev. Med. Chem*., 2004, **4**, 41–48; (b) Y. Adachi, J. Yoshida, Y. Kodera, A. Katoh, J. Takada and H. Sakurai, *J. Med. Chem.*, 2006, **49**, 3251-3256; (c) M. Melchior, K. H. Thompson, J. M. Jong, S. J. Rettig, E. Shuter, V. G. Yuen, Y. Zhou, J. H. McNeill and C. Orvig, *Inorg. Chem.*, 1999, **38**, 2288-2293; (d) M. Yamaguchi, K. Wakasugi, R. Saito, Y. Adachi, Y. Yoshikawa, H. Sakurai and A. Katoh, *J. Inorg. Biochem*., 2006, **100**, 260-269; (e) D. C. Crans, M. Mahroof-Tahir, M. D. Johnson, P. C. Wilkins, L. Yang, K. Robbins, A. Johnson, J. A. Alfano, M. E. Godzala, L. T. Austin and G. R. Willsky, *Inorg. Chim. Acta*, 2003, **356**, 365-378; (f) S. Karmaker, T. K. Saha, Y. Yoshikawa, H. Yasui and H. Sakurai, *J. Inorg. Biochem*., 2006, **100**, 1535-1546.

(43) (a) H. Sakurai, Y. Yoshikawa and H. Yasui, *Chem. Soc. Rev*., 2008, **37**, 2383-2392; (b) N. Domingues, J. Pelletier, C.-G. Ostenson and M. M. C. A. Castro, *J. Inorg. Biochem.,* 2014, **131**, 115-122; (c) J. Pelletier, N. Domingues, M. M. C. A. Castro and C.-G Östenson, *J. Inorg. Biochem.,* 2016, **154**, 29-34.

(44) M. J. M. Campbell, *Coord. Chem. Rev*., 1975, **15***,* 279-319.

(45) S. Padhye and G. B. Kauffman, *Coord. Chem. Rev.*, 1985, **63**, 127-160.

(46) D. X. West, A. E. Liberta, S. B. Padhye, R. C. Chikate, P. B. Sonawane, A. S. Kumbhar and R. G. Yerande, *Coord. Chem. Rev.*, 1993, **123**, 49-71.

(47) D. L. Klayman, J. P. Scovill, J. F. Bartosevich and J. Bruce, *J. Med. Chem.*, 1983, **26**, 39-42.

(48) J. S. Casas, M. S. García-Tasende and J. Sordo, *Coord. Chem. Rev*., 2000, **209**, 197-261.

(49) D. R. Smith, *Coord. Chem. Rev*., 1997, **164**, 575-666.

(50) E. W. Ainscough, A. M. Brodie, J. D. Ransford and J. M. Waters, *J. Chem. Soc., Dalton Trans.*, 1997, 1251-1256.

(51) M. A. Ali, A. H. Mirza, A. M. S. Hossain and M. Nazimuddin, *Polyhedron*, 2001, **20**, 1045-1052.

(52) M. Baldini, M. B. Ferrari, F. Bisceglie, G. Pelosi, S. Pinelli and P. Tarasconi, *Inorg. Chem*., 2003, **42**, 2049-2055.

(53) M. B. Ferrari, F. Bisceglie, G. Pelosi, P. Tarasconi, R. Albertini, G. G. Fava and S. Pinelli, *J. Inorg. Biochem.*, 2002, **89**, 36-44.

View Article Online
DOI: 10.1039/C8DT01668B

(54) M. B. Ferrari, F. Bisceglie, G. Pelosi, P. Albertini, P. P. Dall'Aglio, A. Bergamo, G. Sava and S. Pinelli, *J. Inorg. Biochem.*, 2004, **98**, 301-312.

(55) Saswati, R. Dinda, C. S. Schmiesing, E. Sinn, Y. P. Patil, M. Nethaji, H. S. Evans and R. Acharyya, *Polyhedron*, 2013, **50**, 354-363.

(56) J. Benítez, A. Cavalcanti de Queiroz, I. Correia, M. Amaral Alves, M. S. Alexandre-Moreira, E. J. Barreiro, L. Moreira Lima, J. Varela, M. González, H. Cerecetto, V. Moreno, J. C. Pessoa and D. Gambino, *Eur. J. Med. Chem.*, 2013, **62**, 20-27.

(57) M. Fernández, L. Becco, I. Correia, J. Benítez, O. E. Piro, G.A. Echeverria, A. Medeiros, M. Comini, M. L. Lavaggi, M. González, H. Cerecetto, V. Moreno, J. C. Pessoa, B. Garat and D. Gambino, *J. Inorg. Biochem*., 2013, **127**, 150-160.

(58) B. Demoro, R. F. M. Almeida, F. Marques, C. P. Matos, L. Otero, J. C. Pessoa, I. Santos, A. Rodríguez, V. Moreno, J. Lorenzo, D. Gambino and A. I. Tomaz, *Dalton Trans.*, 2013, **42**, 7131-7146.

(59) G. Scalese, J. Benítez, S. Rostán, I. Correia, L. Bradford, M. Vieites, L. Minini, A. Merlino, E. L. Coitiño, E. Birriel, J. Varela, H. Cerecetto, M. González, J. C. Pessoa and D. Gambino, *J. Inorg. Biochem*., 2015, **147**, 116-125.

(60) (a) S. P. Dash, S. Pasayat, S. Bhakat, S. Roy, R. Dinda, E. R. T. Tiekink, S. Mukhopadhyay, S. K. Bhutia, M. R. Hardikar, B. N. Joshi, Y. P. Patil and M. Nethaji, *Inorg. Chem.*, 2013, **52**, 14096-14107; (b) S. P. Dash, A. K. Panda, S. Pasayat, S. Majumder, A. Biswas, W. Kaminsky, S. Mukhopadhyay, S. K. Bhutia and R. Dinda, *J. Inorg. Biochem.*, 2015, **144**, 1-12; (c) S. P. Dash, A. K. Panda, S. Pasayat, R. Dinda, A. Biswas, E. R. T. Tiekink, S. Mukhopadhyay, S. K. Bhutia, W. Kaminsky and E. Sinn, *RSC Adv.*, 2015, **5**, 51852-51867; (d) S. P. Dash, A. K. Panda, S. Pasayat, R. Dinda, A. Biswas, E. R. T. Tiekink, Y. P. Patil, M. Nethaji, W. Kaminsky, S. Mukhopadhyay and S. K. Bhutia, *Dalton Trans.*, 2014, **43**, 10139-10156; (e) S. P. Dash, A. K. Panda, S. Dhaka, S. Pasayat, A. Biswas, M. R. Maurya, P. K. Majhi, A. Crochet and R. Dinda, *Dalton Trans*., 2016, **45**, 18292-18307; (f) S. P. Dash, S. Majumder, A. Banerjee, M. F. N. N. Carvalho, P. Adão, J. C. Pessoa, K. Brzezinski, E. Garribba, H. Reuter and R. Dinda, *Inorg. Chem.*, 2016, **55**, 1165-1182; (g) S. P. Dash, S. Roy, M. Mohanty, M. F. N. N. Carvalho, M. L. Kuznetsov, J. C. Pessoa, A. Kumar, Y. P. Patil, A. Crochet and R. Dinda, *Inorg. Chem.*, 2016, **55**, 8407-8421.

(61) R. A. Rowe and M. M. Jones, *Inorg. Synth*., 1957, **5**, 113-116.

(62) Part1: S. Ghosh and S. Purohit, *Indian J. Chem., Sect. A: Inorg., Bio-inorg., Phys., Theor., Anal. Chem*., 1987, **26A**, 131.

View Article Online
DOI: 10.1039/C8DT01668B

(63) S. Purohit, A. P. Koley, L. S. Prasad, P. T. Manoharan and S. Ghosh, *Inorg. Chem.*, 1989, **28**, 3735-3742.

(64) (a) A. D. Becke, *J. Chem. Phys.*, 1993, **98**, 5648–5652; (b) J. P. Perdew, *Phys. Rev. B: Condens. Matter Mater. Phys.*, 1986, **33**, 8822-8824.

(65) M. J. Frisch, G. W. Trucks, H. B. Schlegel, G. E. Scuseria, M. A. Robb, J. R. Cheeseman, G. Scalmani, V. Barone, B. Mennucci, G. A. Petersson, H. Nakatsuji, M. Caricato, X. Li, H. P. Hratchian, A. F. Izmaylov, J. Bloino, G. Zheng, J. L. Sonnenberg, M. Hada, M. Ehara, K. Toyota, R. Fukuda, J. Hasegawa, M. Ishida, T. Nakajima, Y. Honda, O. Kitao, H. Nakai, T. Vreven, J. A., Jr. Montgomery, J. E. Peralta, F. Ogliaro, M. Bearpark, J. J. Heyd, E. Brothers, K. N. Kudin, V. N. Staroverov, T. Keith, R. Kobayashi, J. Normand, K. Raghavachari, A. Rendell, J. C. Burant, S. S. Iyengar, J. Tomasi, M. Cossi, N. Rega, J. M. Millam, M. Klene, J. E. Knox, J. B. Cross, V. Bakken, C. Adamo, J. Jaramillo, R. Gomperts, R. E. Stratmann, O. Yazyev, A. J. Austin, R. Cammi, C. Pomelli, J. W. Ochterski, R. L. Martin, K. Morokuma, V. G. Zakrzewski, G. A. Voth, P. Salvador, J. J. Dannenberg, S. Dapprich, A. D. Daniels, Ö. Farkas, J. B. Foresman, J. V. Ortiz, J. Cioslowski and D. J. Fox, *Gaussian 09, revision C.01*; Gaussian, Inc.: Wallingford, CT, 2010.

(66) (a) M. R. Maurya, A. Arya, A. Kumar, M. L. Kuznetsov, F. Avecilla and J. C. Pessoa, *Inorg. Chem.*, 2010, **49**, 6586-6600; (b) M. R. Maurya, M. Bisht, A. Kumar, M. L. Kuznetsov, F. Avecilla and J. C. Pessoa, *Dalton Trans.*, 2011, **40**, 6968-6983; (c) M. R. Maurya, C. Haldar, A. Kumar, M. L. Kuznetsov, F. Avecilla and J. C. Pessoa, *Dalton Trans*., 2013, **42**, 11941-11962.

(67) M. Dolg, U. Wedig, H. Stoll and H. Preuss, *J. Chem. Phys*., 1987, **86**, 866-872.

(68) (a) S. Miertuš, E. Scrocco and J. Tomasi, *Chem. Phys*., 1981, **55**, 117-129; (b) V. Barone and M. Cossi, *J. Phys. Chem. A*, 1998, **102**, 1995-2001; (c) G. Scalmani and M. J. Frisch, *J. Chem. Phys.*, 2010, **132**, 114110.

(69) (a) G. H. Wertz, *J. Am. Chem. Soc.*, 1980, **102**, 5316–5322; (b) J. Cooper and T. Ziegler, *Inorg. Chem.*, 2002, **41**, 6614-6622.

(70) (a) R. Ditchfield, *Mol. Phys*., 1974, **27**, 789-807; (b) K. Wolinski, J. F. Hinton and P. Pulay, *J. Am. Chem. Soc*., 1990, **112**, 8251-8260.

(71) (a) S. Gorelsky, G. Micera and E. Garribba, *Chem. Eur. J.*, 2010, **16**, 8167–8180; (b) G. Micera and E. Garribba, *Dalton Trans*., 2009, 1914-1918; (c) G. Micera and E.Garribba, *J. Comput. Chem.*, 2011, **32**, 2822–2835; (d) G. Micera and E. Garribba, *Eur. J. Inorg. Chem.*, 2011, 3768-3780; (e) D. Sanna, P. Buglyó, L. Bíró, G. Micera and E. Garribba, *Eur. J. Inorg. Chem*., 2012, 1079-1092; (f) D. Sanna, P. Buglyo, A. I. Tomaz, J. C. Pessoa, S. Borovic, G. Micera and E.

View Article Online
DOI: 10.1039/C8DT01668B

Garribba, *Dalton Trans*., 2012, **41**, 12824-12838; (g) D. Sanna, L. Bíró, P. Buglyó, G. Micera and E. Garribba, *J. Inorg. Biochem*., 2012, **115**, 87-99.

(72) A. E. Reed, L. A. Curtiss and F. Weinhold, *Chem. Rev*., 1988, **88**, 899-926.

(73) *CrysAlis PRO*. Agilent Technologies, Yarnton, Oxfordshire, England, 2011.

(74) (a) SMART and SAINT; Bruker AXS, Inc.: Madison, WI, 1996.; (b) Sheldrick, G. M. SADABS; University of Göttingen: Göttingen, Germany, 1996.

(75) (a) G. M. Sheldrick, *Acta Crystallogr*., 2008, **A64**, 112–122; (b) G. M. Sheldrick, *Acta Crystallogr*., 2015, **C71**, 3–8; (c) M. C. Burla, R. Caliandro, B. Carrozzini, G. L. Cascarano, C. Cuocci, C. Giacovazzo, M. Mallamo, A. Mazzone and G. Polidori, *J. Appl. Cryst*., 2015, **48**, 306-309.

(76) (a) L. J. Farrugia, *J. Appl. Cryst*., 2012, **45**, 849-854; (b) K. Brandenburg, DIAMOND. Crystal Impact GbR, Bonn, Germany, 2006.

(77) A. L. Spek, *J. Appl. Crystallogr*., 2003, **36**, 7-13.

(78) (a) B. G. Ha, M. Nagaoka, T. Yonezawa, R. Tanabe, J. T. Woo, H. Kato, U. Chung and K. Yakasaki, *J. Nutr. Biochem.*, 2012, **23**, 501-509; (b) W. S. Matthews, J. E. Bares, J. E. Bartmess, F. G. Bordwell, F. J. Cornforth, G. E. Drucker, Z. Margolin, R. J. McCallum, G. J. McCollum and N. R. Vanier, *J. Am. Chem. Soc.*, 1975, **97**, 7006-7014; (c) W. N. Olmstead, Z. Margolin and F. G. Bordwell, *J. Org. Chem*., 1980, **45**, 3295-3299; (d) F. G. Bordwell, *Acc. Chem. Res*., 1988, **21**, 456-463; (e) E. Buncel, K.T. Park, J. M. Dust and R. A. Manderville, *J. Am Chem. Soc.*, 2003, **125**, 5388-5391; (f) D. Ragno, O. Bortolini, G. Fantin, M. Fogagnolo, P. P. Giovannini and A. Massi, *J. Org. Chem.*, 2015, **80**, 1937-1945; (g) R. Baker, M. J. Spillett, J. Chem. Soc. B, 1969, 581-588; (h) B. G. James, G. Pattenden, J. Chem. Soc. Perkin Trans. 1, 1974, 1204-1208; (i) B. G. James, G. Pattenden, J. Chem. Soc. Perkin Trans. 1, 1974, 1195-1204; (j) S. K. Chattopadhyay, D. Chattopadhyay, T. Banerjee, R. Kuroda and S. Ghosh, *Polyhedron*, 1997, **16**, 1925-1930; (k) A. Pérez-Rebolledo, I. C. Mendes, N. L. Speziali, P. Bertani, J. M. Resende, A. F. de Carvalho Alcôntara and H. Beraldo, *Polyhedron*, 2007, **26***,* 1449-1458.

(79) L. Vilas Boas, J. C. Pessoa, *"Vanadium" in Comprehensive Coordination Chemistry***,** (ed. G. Wilkinson, R.D. Gillard, J.A. McCleverty), Pergamon Press, Oxford, 1987, Vol. **3**, pp. 453.

(80) (a) R. Dinda, P. Sengupta, S. Ghosh and T. C. W. Mak, *Inorg. Chem.*, 2002, **41***,* 1684–1688; (b) R. Dinda, P. Sengupta, M. Sutradhar, T. C. W. Mak and S. Ghosh, *Inorg. Chem.*, 2008, **47***,* 5634-5640.

View Article Online
DOI: 10.1039/C8DT01668B

(81) (a) N. A. Lewis, F. Liu and A. A. Holder, *Eur. J. Inorg. Chem*., 2012, 664-677; (b) N. D. Chasteen, *Vanadyl(IV) EPR spin probe. Inorganic and Biochemical Aspects, in: L. J. J. Berliner and J. Reuben, (Eds.), Biological Magnetic Resonance, Plenum Press, New York*, 1981, pp. 53; (c) T. S. Smith, R. LoBrutto and V. L. Pecoraro, *Coord. Chem Rev*., 2002, **228**, 1-18; (d) J. C. Pessoa, M. J. Calhorda, I. Cavaco, I. Correia, M. T. Duarte, V. Felix, R. T. Henriques, M. F. M. Piedade and I. Tomaz, *J. Chem. Soc. Dalton*, 2002, 4407-4415; (e) P. Adão, M. L. Kuznetsov, S. Barroso, A. M. Martins, F. Avecilla and J. C. Pessoa, *Inorg. Chem.,* 2012, **51**, 11430-11449.

(82) B. K. Koo, Y. J. Jang and U. Lee, *Bull. Korean Chem. Soc*., 2003, **24**, 1014-1016.

(83) C. R. Kowol, N. V. Nagy, T. Jakusch, A. Roller, P. Heffeter, B. K. Keppler and E. A. Enyedy, *J. Inorg. Biochem*., 2015, **152**, 62-73.

(84) A. W. Addison, T. N. Rao, J. Reedijk, J. van Rijn and G. C. Verschoor, *J. Chem. Soc. Dalton Trans*., 1984, 1349-1356.

(85) M. Ishiki and A. Klip, *Endocrinology* 2005, **146***,* 5071-5078.

(86) (a) M. W. Makinen, M. J. Brady, J. Biol. Chem., 2002, 277, 12215–12220; (b) S. S. Amin, K. Cryer, B. Zhang, S. K. Dutta, S. S. Eaton, O. P. Anderson, S. M. Miller, B. A. Reul, S. M. Brichard, D. C. Crans, *Inorg. Chem.* 2000, **39***,* 406-416.

(87) G. Scalese, I. Correia, J. Benítez, S. Rostán, F. Marques, F. Mendes, A. P. Matos, J. C. Pessoa and D. Gambino*, J. Inorg. Biochem*., 2017, **166**, 162-172.

(88) A. M. Ramadan, *J. Inorg. Biochem*., 1997, **65**, 183-189.

(89) (a) P. G. Avaji, C. H. V. Kumar, S. A. Patil, K. N. Shivananda and C. Nagaraju, *Eur. J. Med. Chem.*, 2009, **44**, 3552-3559; (b) J. C. Pessoa, I. Tomaz, *Curr. Med. Chem*., 2010, **17**, 3701-3738; (c) I. Correia et al., *Chem-Asian J.*, 2017, **12**, 2062-2084.

(90) T. Rosu, E. Pahontu, S. Pasculescu, R. Georgescu, N. Stanica, A. Curaj, A. Popescu and M. Leabu, *Eur. J. Med. Chem*., 2010, **45**, 1627-1634.

(91) (a) S. K. Ghosh, R. Saha and B. Saha, *Res. Chem. Intermed.*, 2015, **41**, 4873–4897; (b) Q. Wang, T.T. Liu, Y. Fu, K. Wang and X.G. Yang, *J. Biol. Inorg. Chem.*, 2010, **15**, 1087-1097.